Cloud-Nucleating Particles over the Southern Ocean in a Changing Climate

Cynthia H. Twohy[1,3], Paul J. DeMott[2], Lynn M. Russell[3], Darin W. Toohey[4], Bryan Rainwater[4], Roy Geiss[2], Kevin J. Sanchez[3,5,6], Savannah Lewis[3], Greg Roberts[3,7], Ruhi S. Humphries[8], Christina McCluskey[9], Kathryn Moore[2], Paul W. Selleck[8], Melita D. Keywood[8], Jason P Ward[8], Ian M McRobert[10]

[1]NorthWest Research Associates, Redmond, WA 98052, USA

[2]Colorado State University, Fort Collins, CO 80523, USA

[3]Scripps Institution of Oceanography, University of California, San Diego, CA 92093, USA

[4]University of Colorado, Boulder, CO 80309, USA

[5]NASA Langley Research Center, Hampton, VA 23666, USA

[6]Universities Space Research Association, Columbia, MD, 21046, USA

[7]Centre National de Recherches Météorologiques, Météo-France/CNRS, UMR 3589, Toulouse, France

[8]Climate Science Centre, CSIRO Oceans and Atmosphere, Aspendale, Australia

[9]National Center for Atmospheric Research, Boulder, CO 80307, USA

[10]Engineering and Technology Program, CSIRO Oceans and Atmosphere, Hobart, Australia

Corresponding author: Cynthia H. Twohy (twohy@nwra.com)

Key Points:

- Biogenic sulfate dominates the number concentration of 0.1-0.5 microns diameter particles and CCN over the summertime Southern Ocean
- Biogenic organics are a key component of ice nucleating particles over the Southern Ocean
- As Antarctic climate changes, increased biological activity could partially offset warming effects of sea-ice loss via influences on CCN

Abstract

Stratocumulus clouds over the Southern Ocean have fewer droplets and are more likely to exist in the predominately supercooled phase than clouds at similar temperatures over northern oceans. One likely reason is that this region has few continental and anthropogenic sources of cloud-nucleating particles that can form droplets and ice. In this work, we present an overview of aerosol particle types over the Southern Ocean, including new measurements made below, in and above clouds in this region. These measurements and others indicate that biogenic sulfur-based particles >0.1 μm diameter contribute the majority of cloud condensation nuclei number concentrations in summer. Ice nucleating particles tend to have more organic components, likely from sea-spray. Both types of cloud nucleating particles may increase in a warming climate likely to have less sea ice, more phytoplankton activity, and stronger winds over the Southern Ocean near Antarctica. Taken together, clouds over the Southern Ocean may become more reflective and partially counter the region's expected albedo decrease due to diminishing sea ice. However, detailed modeling studies are needed to test this hypothesis due to the complexity of ocean-cloud-climate feedbacks in the region.

1 Introduction

The concentrations of many aerosol types over Southern Hemisphere oceans are lower than over Northern Hemisphere oceans [*Heintzenberg et al.*, 2000] due to fewer anthropogenic and continental sources. Many of these particles act to nucleate clouds, either as liquid droplets or ice. Low-level marine clouds are especially susceptible to changes in cloud condensation nuclei (CCN) because of their typically small droplet concentrations [*Platnick and Twomey*, 1994]. Approximately 90% of the Southern Ocean (SO) is covered by clouds [*Eastman et al.*, 2014], especially low clouds that are radiatively important, but not well represented in global climate simulations [*Trenberth and Fasullo*, 2010; *J E Kay et al.*, 2016]. SO clouds also are more likely to be supercooled than at similar temperatures in the Northern Hemisphere [*Huang et al.*, 2012], with models overestimating glaciated cloud amount [*J Kay et al.*, 2016]. Thus, the properties of ice nucleating particles (INPs) are also of interest.

The ability of an aerosol particle to grow into a cloud droplet depends largely on its size, mass and water-affinity of hygroscopic material, and the environmental conditions. Over the SO far from anthropogenic pollution, there are two dominant types of CCN: sea spray and bubble-generated particles emitted directly from wind-driven disturbance of the ocean surface ("primary" formation) and marine biogenic particles created through condensation of gas-phase precursors ("secondary" formation). These two CCN types will be referred to in this paper as SS-CCN and MB-CCN, respectively.

SS-CCN are composed of inorganic elements present in bulk seawater, as well as organic material (in bulk seawater and that which consolidates in the sea surface microlayer) that may be present as a surface-active film on the particle surface [*Blanchard*, 1964; *Middlebrook et al.*, 1998]. SS-CCN can range in size from <0.1 μm to 10s of μm in diameter [*Gong*, 2003] and may be an important SO CCN source [*Pierce and Adams*, 2006], particularly in winter months when biological activity is low [*Vallina et al.*, 2006; *Gras and Keywood*, 2017].

SS-CCN are mainly related to windspeed near the ocean surface, with changes in sea-spray aerosol possible even in the pre-industrial climate due to windspeed variations on interannual and decadal time scales [*Xu et al.*, 2015] A 39-year record of wind speeds at Macquarie Island (55°S) showed that surface wind speeds have been increasing at a rate of about 4 cm/s/year at that site [*Hande et al.*, 2012]. More recently, *Young and Ribal* [2019] used a 33-year satellite record to show that mean low-level windspeeds are increasing over the SO at a greater rate (~2 cm/s/yr) than anywhere else on earth. Extreme winds were shown to be increasing even more rapidly, at ~5 cm/s/yr. *Korhonen et al.* [2010] calculated that the wind-

driven increases in sea-spray CCN number between 1980/82 to 2000/02 were sufficient to counteract expected radiative forcing changes due to greenhouse gas emissions and ozone loss in the 50-60°S latitude zones.

MB-CCN can be composed of both sulfur and carbonaceous compounds. MB-CCN over the remote oceans originate primarily from biological gases lofted into the troposphere, where they form new particles and grow by condensation and coagulation to CCN sizes [*Bates et al.*, 1998; *Clarke and Kapustin*, 2002; *Quinn et al.*, 2017]. Gas to particle conversion is thought to occur mostly through a dimethyl sulfide (DMS) to methane sulfonic acid (MSA) or sulfur dioxide vapor to sulfuric acid or MSA aerosol pathway [*Chen et al.*, 2018]. Conversion of the particles to ammonium bisulfate or sulfate may then occur when sufficient ammonia vapor is present. New particle formation may be aided by the presence of iodine [*O'Dowd et al.*, 2002; *Saiz-Lopez et al.*, 2007], organics [*Donahue et al.*], mercury [*Humphries et al.*, 2015], or ions [*Yu and Gan*, 2010; *Jokinen et al.*, 2018]

During the austral spring and summer, favorable phytoplankton growth conditions of minimal sea ice, warmer temperatures, and enhanced light [*Petrou and Ralph*, 2011] lead to "blooms" which enhance biological emissions to the atmosphere. Nutrients and diatoms released in the spring from melting sea ice and icebergs [*Smetacek and Nicol*, 2005] and ocean circulation changes favoring enhanced upwelling in summer months also contribute important raw ingredients for phytoplankton growth [*Tremblay and Gagnon*, 2009]. Over the Southern Hemisphere oceans, the approximately 3-fold increase in CCN concentrations between winter and summer months [*Boers et al.*, 1998] is mostly due to MB-CCN produced from ocean phytoplankton emissions [*Vallina et al.*, 2006; *Korhonen et al.*, 2008; *Gras and Keywood*, 2017].

This summertime increase in MB-CCN number has been observed to elevate SO stratocumulus cloud droplet concentration and lower droplet effective radius; the calculated enhancement in cloud albedo for the same liquid water path [*Boers et al.*, 1998] would result in less shortwave radiation reaching the surface. *McCoy et al.* [2015] found that ocean chlorophyll-a was correlated with cloud droplet number over the ocean at 35-55°S latitudes and also inferred that MB-CCN had a strong influence cloud albedo. *Engström et al.* [2015] measured positive perturbations in cloud albedo at higher southern latitudes that aligned with areas of high ocean chlorophyll. Chlorophyll-a concentrations during phytoplankton blooms over the SO were also related to a reduction in precipitation, presumably due to enhanced MB-CCN producing smaller droplet sizes [*Krüger and Graßl*, 2011].

Recent ocean modelling studies predict myriad impacts on ocean biota at polar latitudes in a warming climate. Predicted climate changes in the Southern Ocean region may influence marine nutrient transport [*Moore et al.*, 2018], ocean uptake of CO_2 [*Gray et al.*, 2018] and

ocean acidification [*Westwood et al.*, 2018]. If phytoplankton populations change in the future, so may concentrations of cloud nucleating particles and cloud properties.

Some recent global modelling studies predict changes in CCN and cloud properties in response to prescribed changes in phytoplankton loadings (e.g., [*Wang et al.*, 2018]), and have implemented marine biogenic CCN parameterizations based on simulated monthly mean concentrations of ocean surface biogenic constituents [*Wang et al.*, 2020]. While simulations indicate these biogenic CCN may impact simulated cloud radiative forcing over the Southern Ocean [*Zhao et al.*, 2020], work remains in incorporating expected ocean biota changes in this region and in carefully evaluating the cloud-nucleating particles against observations. For example, *Schmale et al.* [2019] presented elevated MSA and CCN concentrations over high chlorophyll regions near Antarctica and found that even the GLOMAP aerosol process model underestimated CCN by over 50% in the region. Additionally, coupled ocean-atmosphere simulations targeted at investigating future phytoplankton loadings highlight complex interactions between biological activity, cloud-nucleating particles, cloud occurrence and albedo, and mineral dust (nutrient) deposition over the southern hemisphere that are not currently fully elucidated [*Gunson et al.*, 2006], motivating further investigations of complex Southern Ocean region's response to warming.

Ocean biological activity also can be an important source of INPs in some environments. *Vergara-Temprado et al.* [2018] calculated that low INP concentrations over the SO are a major factor in maintaining supercooled clouds there, with important radiative impacts. Prior to The Southern Ocean Clouds, Radiation, Aerosol Transport Experimental Study (SOCRATES) campaign described here, observations of SO INP number concentrations were limited to ship-based measurements [*Bigg*, 1973; *McCluskey et al.*, 2018b]. The latter study documented low INP concentrations over the SO compared to continental regions and that INPs within the marine boundary layer (MBL) were dominated by marine sources. There are at least two types of marine INPs that can nucleate ice at the relatively warm temperatures (T>~255K) prevalent in SO low-level clouds. Microbes such as bacteria, viruses and diatom fragments can be lofted into the atmosphere directly and act as INPs [*Bigg and Leck*, 2008; *Després et al.*, 2012; *McCluskey et al.*, 2018a]. In addition, smaller organic biomolecules that have INP properties can be produced in bubble bursting from jet drops containing bulk seawater or from film drops more representative of the composition of the sea-surface microlayer [*Wilson et al.*, 2015; *McCluskey et al.*, 2018a]. These types of biogenic INPs are expected to dominate INP number at low altitudes over remote marine regions like the Southern Ocean [*Burrows et al.*, 2013; *McCluskey et al.*, 2018b] and may be co-emitted with inorganic seawater components. Mineral dust is another important INP type that nucleates ice more efficiently than marine aerosol for a given aerosol surface area at temperatures colder than about 263K (e.g., DeMott et al., 2016). Dust is present in much lower concentrations

over the SO relative to the tropical and northern oceans [*Heintzenberg et al.*, 2000; *Jickells et al.*, 2005], so that the productivity of SO phytoplankton tends to be iron limited except in upwelling regions [*Jickells et al.*, 2005]. Despite relatively low dust concentrations, modelling studies that predicted Southern Ocean INPs associated with simulated marine and dust aerosol found that even small amounts of dust aerosol transported from far distances may serve as an important source to Southern Ocean INP populations at cloud relevant altitudes [*McCluskey et al.*, 2019].

In this paper, we present new atmospheric aerosol measurements that support oceanic phytoplankton as a significant source of both primary and secondary SO cloud nucleating particles. We then use these and other SOCRATES results, as well as those from past experiments and published modelling studies, to discuss ways in which these particles could change and influence cloud properties in a future climate.

2 Experiment

SOCRATES was conducted with the National Science Foundation's Gulfstream-V aircraft in the austral summer, January and February of 2018. The aircraft flew south from Tasmania in Australia, typically conducting a survey leg southbound at about 6 km altitude, then returning northbound with ten-minute legs at 150 m above the ocean surface, within low-level layer clouds, and about 300 m above the cloud tops. Aircraft measurements covered about 49°S to 61°S latitudes, where a variety of windspeed and cloud temperature regimes and warm, supercooled, mixed-phase, and fully glaciated clouds were encountered. Temperatures of the low level clouds sampled by the aircraft ranged from about 253K to 283K. Shipboard measurements extended farther south to the Antarctic ice shelf through the associated CAPRICORN-2 cruise on the RV *Investigator* during the same period. During summer months, sea ice retreats almost to the Antarctic continent at the longitudes south of Australia [*Frey et al.*, 2018]. Figure 1 shows the location of the SOCRATES flight tracks, as well as the CAPRICORN-2 cruise data, superimposed on ocean chlorophyll-a concentration from the MODIS satellite sensor.

Aerosol impactor samples in cloud nucleating size ranges were collected in clear air below clouds (at 150 m above the ocean surface) and in the free troposphere above clouds. Cloud residual particles were also collected in clouds using a Counterflow Virtual Impactor (CVI) inlet [*Noone et al.*, 1988]. In cloud, the CVI rejects interstitial aerosol using a dry counterflow airstream, while collecting and evaporating droplets which are then evaporated so individual non-volatile droplet residuals are collected. The CVI inlet and porous tube were composed of titanium and the sample lines were stainless steel. The CVI inlet was heated to ~50°C during cloud sampling in order to evaporate cloud droplets, and the sample

stream was maintained at 40°C to prevent condensation prior to measuring the associated water vapor with a tunable diode laser hygrometer. Ambient aerosol particles were collected below and above cloud by periodically turning off the CVI counterflow airstream and heaters to minimize losses of volatile species during sample collection. Particles were collected with a two-stage impactor onto carbon-coated electron microscope grids (for elemental analysis) and onto silicon nitride membrane windows (for organic functional groups) in two dry diameter ranges of about 0.1-0.5 μm and 0.5-5 μm. (These physical diameters assume spherical particles with densities of 2 g cm^{-3} at 1000 mb.) Impactor substrates were stored immediately after flights and held for off-line analysis below 0°C.

The single-particle elemental composition of selected samples was measured via analytical Scanning Transmission Electron Microscopy (STEM) using Energy Dispersive X-ray Spectroscopy (EDS) at Colorado State University; these results are presented in Sections 3.1.1 and 3.1.3. Organic functional groups in single particles were analyzed via a different technique, Soft X-ray Scanning transmission X-ray microscopy (STXM) using Near-Edge X-ray Absorption Fine Structure (NEXAFS), at the Lawrence Berkeley National Laboratory; these results are presented in Section 3.3. Technique and categorization for the STEM and STXM analysis are described further in the Supporting Information. Samples from clouds or ambient air containing drizzle or ice were not analyzed due to the possibility of breakup producing spurious particles [*Twohy et al.*, 2003; *Craig et al.*, 2013], which biases our in-cloud samples toward non-precipitating clouds. Figure 1 (left) shows the location of the below-cloud, in-cloud and above-cloud single-particle samples used in our Figure 2 analysis.

Ice nucleating particles were measured directly with a continuous flow diffusion chamber CFDC-1H [*DeMott et al.*, 2015]. The aircraft-based CFDC sampled from the HIAPER modular inlet outside of cloud and the CVI inlet within clouds to enhance INP detection limits. A pre-impactor with a 50% cut size of 2.5 μm aerodynamic diameter was also employed to assure discrimination of ice crystals grown within the CFDC from larger aerosol particles. INPs were also measured with a CFDC aboard the RV *Investigator* in CAPRICORN-2, and for that instrument an aerosol concentrator and a 1.5 μm pre-impactor was used (see Supporting Information). Ice crystals grown in the CFDCs and their associated INPs were collected with a single-stage impactor (4.0 μm aerodynamic diameter) onto similar substrates and their residuals were analyzed via the same single-particle techniques as for the below cloud, in-cloud residuals and above cloud particles. Figure 1 (right) shows the location of the ice nucleating particle samples used in our analysis and compiled in Section 3.2. Wing and cabin-mounted Ultra-High Sensitivity Aerosol Spectrometers (UHSAS, 0.06-1 μm diameter, Droplet Measurement Technologies) were also used for aerosol size distribution measurements aboard the aircraft.

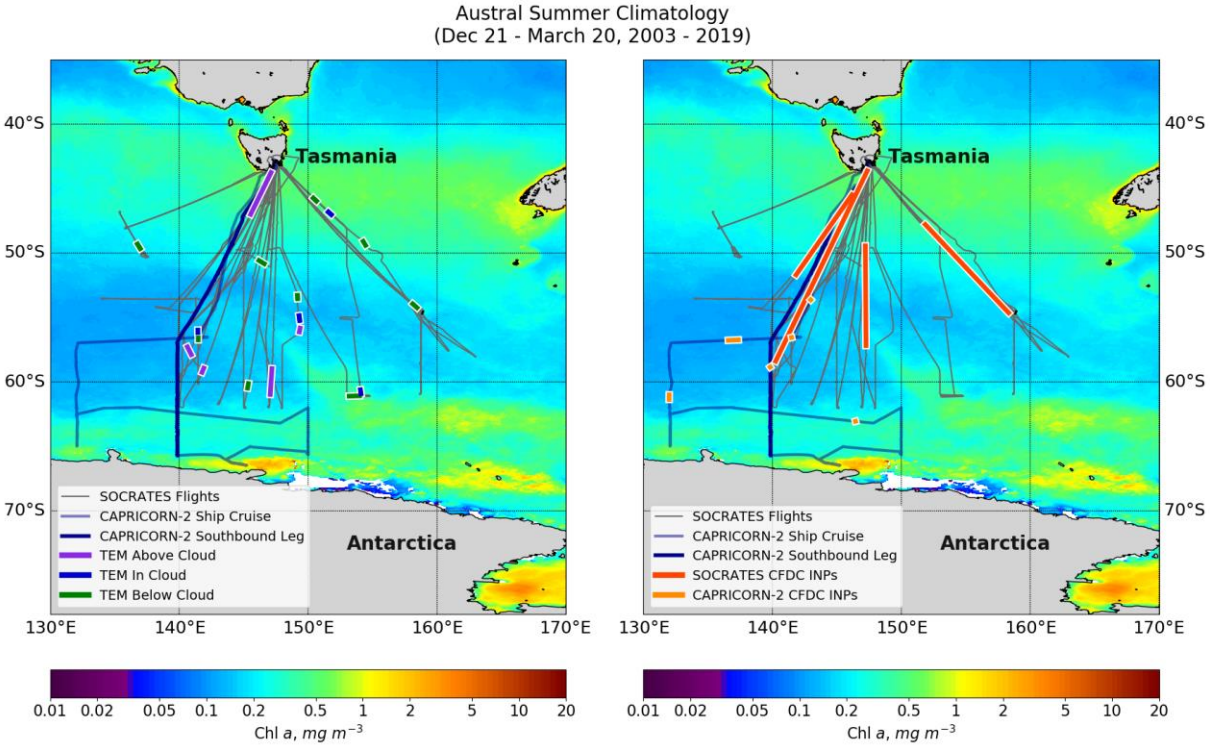

Figure 1. SOCRATES aircraft flight tracks (dark green lines) and CAPRICORN-2 ship cruise (blue lines) over the Southern Ocean in 2018. These are superimposed on ocean chlorophyll-a concentrations from the MODIS instrument on the Aqua satellite for 2003-2019 during austral summer (Dec 21-Mar 20). The bold part of the ship track shows the southbound track latitudes with chemical data shown in Table 1. On the left, locations of the aircraft STEM single-particle samples are shown in purple, blue and green, for above cloud, in cloud and below cloud, respectively. On the right, locations of the INPs collected behind the CFDC instrument are shown for the aircraft samples in red and for the ship samples in orange.

Other measurements on the RV *Investigator* included in this work were bulk aerosol composition and cloud condensation nuclei (CCN) concentration. The aerosol observation capability onboard the RV *Investigator* is briefly described in *Humphries et al.* [2019]. Aerosols were sampled via an inlet located 18.4 m above sea level. A Time-of-Flight Aerosol Chemical Speciation Monitor (ToF-ACSM, Aerodyne Research) was used to determine the chemical composition of aerosols between 0.04 μm and 1 μm diameter, although transmission of <0.1 μm particles is less than 100% [*Fröhlich et al.*, 2013]. More information on the handling of ToF-ACSM data can be found in the Supporting Information.

Concentrations of cloud condensation CCN were measured using a continuous-flow streamwise thermal-gradient CCN counter (CCNC, Model CCN-100, Droplet Measurement Technologies).

3 Results

3.1 Aerosol Particle Composition

3.1.1. Elemental Composition of Single 0.1-0.5 μm Aerosol Particles

In this section, the composition of single particles in the 0.1-0.5 μm diameter size range at different altitudes is presented. Marine CCN number concentration at cloud relevant supersaturations is dominated by particles smaller than 0.5 μm diameter because they are more abundant than larger particles [*O'Dowd et al.*, 1997a]. However, the minimum size of particles activated into droplets can vary with environmental conditions and aerosol particle composition. To assess the representativeness of the 0.1-0.5 μm population as CCN for SOCRATES, the mean number concentrations of particles 0.1 μm to 1.0 μm during the below-cloud sample periods were compared to the mean cloud droplet number concentration in the nearest low cloud leg. The wing-mounted UHSAS was used for the aerosol concentration measurement or, if those data were not available, the rack-mounted UHSAS behind the CVI was used. The 0.1 μm to 1.0 μm number concentration ranged from 71% to 194% (median 98%) of the cloud droplet number concentration (which varied from 31 cm^{-3} to 207 cm^{-3}). Also, the particle number concentration between 0.5 μm and 1.0 μm was a small fraction (typically ~5%) of the total number concentration between 0.1 μm and 1.0 μm. Thus barring significant coalescence, particles in the 0.1 to 0.5 μm diameter range were representative of the CCN population in many clouds over the SO.

Figure 2a shows the fraction by number of different particle composition types measured for the 0.1-0.5 μm diameter SOCRATES particle population. (Figure 2b shows the >0.5 μm particle population, which will be discussed later in section 3.1.3). Mean values for three different types of samples are included, those below cloud at about 150 m above the ocean surface, in-cloud residual particles, and above clouds.

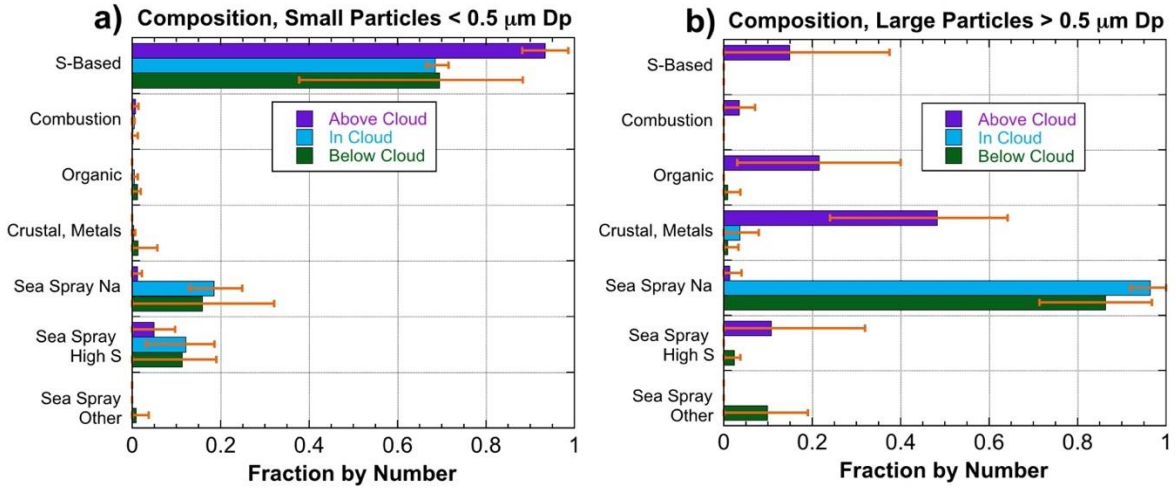

Figure 2. a) Fraction by number of different particles ~0.1-0.5 μm dry diameter sampled below cloud at 150 m altitude (green), within cloud droplets (blue) and in the free troposphere (purple) as measured by STEM (details in Supporting Information Text S1 and Table S1). Color bars are the means of all samples from different flights. Orange bars represent the range for *n* individual samples (below cloud: *n*=6; in-cloud: *n*=3; above cloud: *n*=2). Since particles in this size range were found to be partially volatile with the CVI heaters on, 150 m and above cloud samples were only analysed for later flights (#11-#15) when heaters were turned off. 791 particles total are included. b) Fraction by number of different particles ~0.5-5 μm dry diameter sampled at 150 m (green), within cloud droplets (blue) and in the free troposphere (purple). Color bars are the means of all samples from different flights. Orange bars represent the range for *n* individual samples (below cloud: *n*= 6; in-cloud: *n*=3; above cloud: *n*=3). 364 particles total in the large size range were analyzed.

The 0.1-0.5 μm diameter particles were dominated by sulfur-based particles, with the highest number fraction of these in the above-cloud aerosol (Figure 2a). These particles are also likely to have some organic components that cannot be detected by STEM for these small particle sizes [*Saliba et al.*, 2020], particularly if they are volatile. However, based on the consistently high sulfate to organic mass content presented later from the ship-board ToF-ACSM data (Table 1), we expect sulfate to be present at higher mass levels than organics in the >0.1 μm particles, which represent most of the sub-micron particle mass and much of the accumulation mode number. The second-most frequent particle type in this size range was defined as sodium-based sea-spray (SS), which was most numerous at 150 m and in cloud residuals. There were two types of sodium-based sea spray: particles comprised of mostly

NaCl (with other inorganic and organic sea-spray components), and those in the sea-spray "high S" category, which also had sodium but were enriched in sulfur and depleted in chlorine due to uptake and condensation of sulfur gases [*McInnes et al.*, 1994]. Almost half of the SS particles in this smaller size range had sulfur enrichment. The mean composition for 3 in-cloud residual samples in this size range was 68% sulfur-based and 31% for sea-spray. These measured in-cloud ratios are consistent with compositional CCN number fraction at 0.2-0.3% critical supersaturation as calculated from aerosol data by *Quinn et al.* [2017]'s Figure 4a, as well as the summer biogenic CCN fractions calculated by *Gras and Keywood* [2017] and *Fossum et al.* [2018]. SS-based particles were detected by the STEM down to 0.1 μm in diameter, but were larger overall, with median measured diameters of 0.28 μm vs 0.18 μm for the S-based particles in size-resolved below-cloud samples. While substantially more droplets activate on S-based particles than on SS in this size range in summertime SO clouds, SS may be important in influencing peak cloud supersaturation and thereby cloud droplet number [*Fossum et al.*, 2020]. Externally mixed organics, high K-combustion particles, and crustal (mineral) dust and metals were detected in the <0.5 μm population at various heights, but at less than 3% by number.

For the 150 m particles, some variation in composition was seen from case to case [*McFarquhar et al.*, 2020], but in all but one of the six cases, sea-spray was secondary in number to sulfur-based particles. The dominance of sulfur-based particles in the 0.1-0.5 μm size range (and thus as CCN that influence cloud droplet number) is expected in the spring and summer months over the SO. As discussed in the Introduction, favorable conditions for phytoplankton growth leads to enhanced biological sulfur emissions and nucleation of new particles, often in the cold, clean free troposphere. Nucleation is usually suppressed within the warmer MBL where pre-existing sea-spray surface area is high. *McCoy et al.* [2021] found that at the latitudes probed by the SOCRATES aircraft, enhanced concentrations of small (0.01-0.08 μm) particles were frequently observed aloft over a wide area of the free troposphere, often in airmasses having undergone convective uplift. Those observations support the theory of secondary particle formation occurring in the free troposphere over the world's oceans, where they then grow by condensation and coagulation to CCN sizes before being re-entrained into the marine boundary layer [*Clarke et al.*, 1996; *Bates et al.*, 1998; *Clarke and Kapustin*, 2002; *Quinn et al.*, 2017]. However, as discussed in Section 4.1, the free troposphere may not be the only origin of marine biogenic CCN over the SO.

3.1.2. Submicron aerosol bulk composition

To investigate further the source and composition of sulfur-based aerosol particles in the region, shipboard measurements were used to examine the changes in submicron aerosol mass composition and CCN concentration for different latitude bands. During the same January-February time period as the aircraft measurements, sulfate aerosol mass peaked at latitudes to the north of 50°S and to the south of 62°S (Table 1). This is similar to the latitudinal dependence of chlorophyll-a (Figure 1), and is consistent with biological sources of particles to the north and south of ~50-60°S. CCN concentrations [*Sanchez et al.*, 2021] also peaked in air to the north and south and were highly correlated with sulfate concentrations (r^2=0.77 for 1 hr averages). Ammonium and nitrate mass were both below their detection limits along the track, even for areas with higher sulfate values, consistent with low oceanic sources of ammonia and nitrate [*O'Dowd et al.*, 1997b; *Jokinen et al.*, 2018]. Because of relatively high detection limit for ammonium, the molar ratio of $NH4^{+}/SO4^{2-}$ can't be reliably calculated from these data. However, it can be estimated to be about 0.5 from average $NH4^{+}$ and $SO4^{2-}$ concentrations of 0.042 μg m^{-3} and 0.420 μg m^{-3}, respectively, measured over the summertime SO by [*Xu et al.*, 2013]. This is consistent with an acidic sulfate aerosol with compositions varying between sulfuric acid and ammonium bisulfate [*O'Dowd et al.*, 1997b].

Table 1.

Submicron Aerosol Composition and CCN Number Concentration for 3 Latitude Ranges

Latitude	SO_4^{2-} μg m^{-3}	NH_4^{+} μg m^{-3}	NO_3^{-} μg m^{-3}	Organic μg m^{-3}	MSA μg m^{-3}	CCN 0.3% cm^{-3}
45°S-50°S	0.320 (0.122)	BDL	BDL	BDL	BDL	230 (82)
50°S-62°S	0.112 (0.076)	BDL	BDL	BDL	BDL	116 (55)
62°S-65.7°S	0.352 (0.113)	BDL	BDL	BDL	0.030 (0.014)	241 (65)

Note. Submicron aerosol concentration from shipborne ToF ACSM and CCN number concentration at 0.3% supersaturation from shipborne CCN counter during southbound portion of CAPRICORN-2 ship cruise (14 Jan 2018-1 Feb 2018). Numbers in parenthesis are measurement standard deviations for the latitude range. A collection efficiency of 1.0 was assumed for the ACSM data. *BDL* is below the detection limit of 0.013 μg m^{-3} for sulfate, 0.178 for ammonium, 0.007 for nitrate, and 0.086 for organics, and 0.022 for MSA. MSA was not calibrated specifically for this instrument, but is included to show the increase south of 62°S. See Supporting Information for more ACSM details.

Organic aerosol mass was also usually below its detection limit and was always much lower than sulfate. For brief periods between 45°S -50°S when organic mass was above its detection limit, the sulfate to organic mass ratio was about 0.2, so we consider that to be an upper bound. The dominance of sulfate over organic matter in the summertime SO submicron particles has also been documented by *Fossum et al.* [2018]. In that cruise south of South America, organic matter measured with a ToF aerosol mass spectrometer only comprised 2%-7% of the submicron particle mass. While apparently low over this part of the SO, organic mass can be significant in some marine environments, particularly in maller particles [*O'Dowd et al.*, 2004] which may not contribute much mass [*Saliba et al.*, 2020]. Also, since refractory sea-spray is inefficiently measured by ACSM-type instruments [*Frossard et al.*, 2014], organic mass and excess sulfate on sea-spray particles will be underestimated by this technique.

The response of time-of-flight aerosol mass spectrometers to MSA has been shown to be instrument-specific [*Hodshire et al.*, 2019], so these measurements are used qualitatively. MSA was in the noise until south of 62°S, where it increased to detectable levels and covaried with the sulfate mass (Table 1). Since DMS is the only source of particulate MSA, this indicates increased biogenic activity over recently sea-ice free, upwelling waters near Antarctica. Others have also found that MSA increases at high southern latitudes [*Davison et al.*, 1996; *Heintzenberg et al.*, 2000; *Quinn et al.*, 2000; *Xu et al.*, 2013], and it has been observed to reach up to ~50% of sulfate mass in Antarctic regions during summer [*Read et al.*, 2008; *Chen et al.*, 2012; *Jung et al.*, 2019].

These data, taken together with the high volatility of the SOCRATES submicron aerosol [*McCoy et al.*, 2021] indicate that the ~0.1-0.5 μm particles measured over the SO that comprise most of the CCN number were dominated by biogenically-produced acidic sulfate, probably with some contribution from biogenic MSA and organic material [*Saliba et al.*, 2020]. There is also a smaller but significant contribution to ~0.1-0.5 μm particle number from sodium-based sea-spray, often internally mixed with excess sulfur from atmospheric processing.

3.1.3. Elemental composition of single >0.5 μm aerosol particles

Figure 2b shows that particles in the >0.5 μm size range were dominated by sodium-based sea-spray in the MBL, both below cloud at 150 m and in cloud. Fewer of these larger sea-spray particles showed sulfate enrichment relative to those in the small size range (Figure 2a). This is consistent with their lower surface to volume ratio and longer residence times in the atmosphere for condensation of acidic gases to occur [*McInnes et al.*, 1994; *Song and Carmichael*, 1999], and size-dependent cloud chemistry [*Twohy et al.*, 1989]. Below cloud, about 10% of the large SSA particles were enriched in calcium and/or magnesium. This

enrichment has been noted by others (*Keene et al.* [2007]; [*Gaston et al.*, 2011]; *Salter et al.* [2016]), and is presumed to be due to the presence of coccolith fragments [*Hawkins and Russell*, 2010] or to the binding affinity of cations to organic substances present in the sea surface microlayer [*Jayarathne et al.*, 2016]. Marine aerosols with enhanced magnesium and calcium relative to sodium have also been correlated with periods of enhanced marine biological activity as indicated by chlorophyll-a and DMS [*Gaston et al.*, 2011].

By mapping of elements in individual particles (one example in Figure 3), we found that many of the sea-spray particles in the larger size range had detectable amounts of carbonaceous material surrounding the primary NaCl crystal. This internal mixing of organics with sea-salt has been noted by *Middlebrook et al.* [1998], *Russell et al.* [2010], and others, with the organics thought to be biogenic compounds that are mixed in sea-spray droplets from near the surface ocean. These organic coatings on sea spray particles may be relevant for the INP population, as previous measurements of ice crystal residuals from laboratory-generated sea spray aerosol included crystalline particles with organic coatings, among other particle types [*McCluskey et al.*, 2018a]. The importance of organic material as INPs is supported by our findings of higher number fraction and different functional groups of organic INPs vs. the general population of below-cloud aerosol, discussed in Section 3.2 and 3.3.

The sea-spray coatings shown in Figure 3 were not just carbonaceous, however, but were usually co-located with magnesium and oxygen. Crystals of calcium, sulfur and oxygen (presumably calcium sulfate) were also observable adjacent to the NaCl crystals and sometimes co-located with the organic matter. Enrichment of Mg^{2+} and Ca^{2+} has been associated with reactions of these cations with biological exudates such as fatty acids in seawater [*Bikkina et al.*, 2019]. The size of organic coatings on sea-spray as observed via STEM was quite variable, and may be related not only to differences in ocean biological activity but also due to relatively strong winds, which are often greater than ~8 m s^{-1} over the SO [*Korhonen et al.*, 2010]. *Gantt et al.* [2011] found that organic mass on sea-spray aerosol was inversely correlated with mean wind speed, since breaking waves at windspeeds >8 m s^{-1} may mix organic material from the sea surface microlayer into the deeper water column. About 1% of the particles measured in both size ranges (0.1-0.5 μm and >0.5 μm) were primarily organic in composition, and about 1/3 of those showed unusual morphology suggestive of primary biological particles or fragments. Based on unpublished fluorescent-based data from a WIBS-4A [*Twohy et al.*, 2016], biological particles were typically about 0.1-1% of the total number of >0.8 μm particles at 150 m over the region sampled, which is consistent with the STEM analysis.

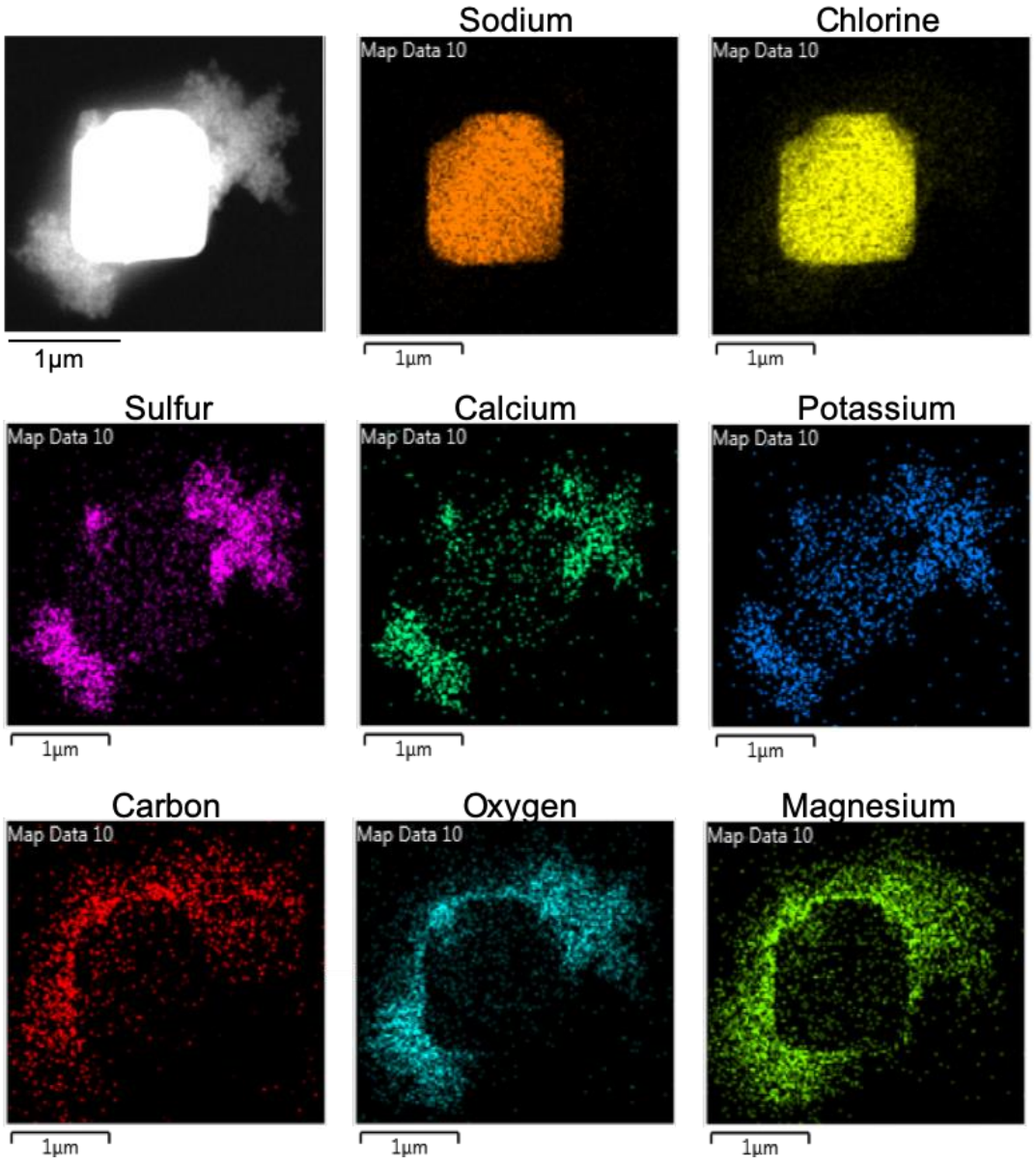

426

427 **Figure 3.** STEM mapping analysis of an individual sea-spray particle sampled from 150 m
428 above the ocean surface during SOCRATES. The colored images show the location of
429 different elements (given at the top of each image) within the particle.

The composition of the large particles in the free troposphere above cloud was very different from that of the MBL aerosol, with substantial variation in composition for the three flights sampled. Though the total number of particles collected was small (n=71), a range of particle types were found above cloud, with mineral dust and metals the most common, followed by organics and sulfur-based, with a small contribution from combustion particles. Thus, this large-particle population in the free troposphere apparently has a substantial contribution from continental aerosol particles from long-range transport. *Froyd et al.* [2020] showed that the Saharan dust can contribute atmospheric dust to regions of the Southern Hemisphere, but *Neff and Bertler* [2015] found that Australia was the primary source region for dust over the SOCRATES flight area, with smaller contributions from southern Africa and New Zealand. In addition, 11% of >0.5 μm particles in the free troposphere were primarily metallic, which may be from Australian mining activities known to emit atmospheric aerosol particles enriched in metals [*Radhi*, 2010]. While the types of metals found varied, the most common metals in all SOCRATES STEM samples were aluminum and copper, which are also elements extensively mined in Australia.

We compared the number concentration of particles in the 0.5-1.0 μm size range (from the UHSAS) for 10-min above-cloud legs vs 150 m legs for five flights that had well developed, single low cloud layers. Particle number concentrations above cloud ranged from about 0.02-0.06 cm^{-3}, and were only 0.5%-3% of concentrations in the same size range at 150 m. Despite the low concentrations of free tropospheric particles in this size range, mineral dust may still represent an important source of free tropospheric INPs for mid-level clouds over the SO [*McCluskey et al.*, 2019]. This is because sea-spray aerosol are much less numerous in the free troposphere, and dust is a more efficient ice nucleator than sea-spray aerosol at temperatures below about 255K [*Murray et al.*, 2012].

3.2. Composition of Ice Nucleating Particles

Six samples of INPs collected behind the CFDC on the ship cruise and four samples from the G-V aircraft were also analyzed via STEM. The samples are expected to be dominated by INPs from the MBL, since the ship only sampled from the MBL and the aircraft sampled more total INPs from the MBL than from higher altitudes. The sizes of collected INPs were measured on the substrates (as imaged from the microscope), and ranged from about 0.1 to 1.5 microns diameter, the largest size accepted due to the sampling configuration as discussed in the Experiment section and in Supporting Information. The CFDC processing temperature ranged from 241K to 246K. Because the number of ice nucleating particles found and analyzed was low (n=87), the compositions of all INP samples were averaged together in Figure 4.

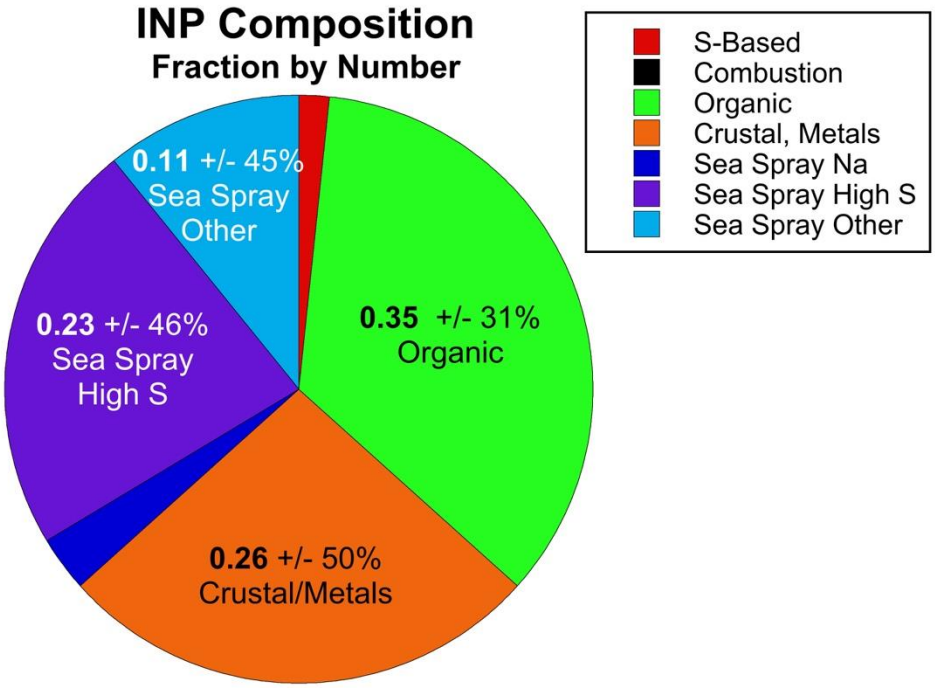

Figure 4. Fractional composition by number of ice nucleating particles collected over the Southern Ocean via shipborne and airborne CFDCs at 241K to 246K processing temperatures and analyzed via STEM. 87 INPs ranging in size from 0.1 to 1.5 µm physical dry diameter are included. Estimated uncertainty in fractional composition varied with particle type and size and is shown as +/- values for the dominant types of INPs.

The results indicate that INPs over the Southern Ocean active were dominated by three types: organics, salt-based sea-spray, and mineral dust/metals. Organics and dust/metals were enhanced relative to their abundance in the ambient MBL aerosol samples. Note that particles in the organic category could also originate from sea-spray, but are not dominated by sodium, calcium or magnesium like the "Sea-Spray Na", "Sea-Spray High S" and Sea-Spray Other" categories. The salt-based sea spray categories may also contain organic coatings conferring INP activity. Over 1/3 of the INPs were mainly organic, with about 1/4 of these having morphologies that likely were primary biological (microbial) particles or fragments. The other 3/4 of the organics were more amorphous but presumably were also generated from the ocean surface by the processes discussed in Section 3.2. The relatively small fraction of microbial particles and relatively higher fraction of mineral dust and metals could be reflective of the lower processing temperatures (241K to 246K) required to collect sufficient numbers of INPs in real-time with the CFDC. In particular, the lower temperature range may

favor other entities that are ice nucleating, such as mineral dust, rather than the microbial particles that may be favored at higher temperatures more representative of most SOCRATES low clouds. While the microbial type was not identified as a major INP type at lower CFDC processing temperatures in SOCRATES, it was identified as contributing at temperatures higher than 253K through heat sensitivity studies of immersion freezing INPs measured from filter-collected particles during CAPRICORN-1 [*McCluskey et al.*, 2018b] and also in filter collections during the Measurements of Aerosols, Radiation and Clouds over the Southern Ocean (MARCUS [*McFarquhar et al.*, 2020] study (Paul DeMott, personal communication). The diversity of marine INP types sampled during SOCRATES and associated CAPRICORN studies supports laboratory studies indicating a range of marine INP types [*McCluskey et al.*, 2018a]. Overall these results are consistent with our present knowledge of the main types of INPs present over remote oceans.

3.3 Organic Functional Groups Present in Aerosol and Ice Nucleating Particles

Six particle samples from 150 m above the ocean, five samples in cloud, and three free tropospheric samples were analysed for organic functional groups via STXM. All except one of these samples were from the large (>0.5 μm) impactor stage, since most of the silicon nitride windows broke under the higher flow velocity required to impact smaller particles. In addition, four samples with ice nucleating particles from the CFDC instrument were analyzed. Two of these INP samples were collected from the G-V aircraft at various flight levels on 2/3/18 and 2/24/18 and two were collected in the MBL from the CAPRICORN-2 ship cruise in the same region on 1/26/18 and 2/18/18. As described in the Supporting Information, approximately 200 particles total of the four sample types (150 m, cloud droplet residuals, above cloud, and INP) were analyzed via STXM for organic functional groups.

Less than half of the 150 m and cloud droplet residual particles had detectable organic functional group peaks above the noise. In contrast, 73% of the INPs included a measurable carbon signal. 102 in total of the particles analyzed had enough carbon to detect organic functional group peaks, but 3 potential INPs were eliminated to their large size. The remaining 99 particles were between 0.15 and 2.7 μm in dry diameter, with a median diameter of 0.74 μm, so larger particles were emphasized in this analysis. Differences in size and organic properties between the different types of samples were assessed by comparing the means and standard deviations for C edge and different organic functional groups for in-cloud, above cloud and INPs with the mean and standard deviation of the 150 m MBL samples. Differences significant at $p \leq 0.05$ were tested using two-tailed t-tests via three different methods as described in the Supporting Information Text S2, with t-values given in Tables S2, S3 and S4.

The sizes of the particles analyzed in cloud, above cloud, and for INPs were not significantly different from the 150 m particles at the 95% probability level. Particles with detectable carbon showed no significant differences in organic content or functional groups between the 22 150-m ambient aerosol samples and 23 cloud residual samples. Total carbon in INPs was 63% higher than for 150-m aerosol particles in the mean, although this difference was not significant at the 95% probability level.

The intensities of individual organic functional groups, however, showed several significant differences between SOCRATES INPs and the 150-m samples. INPs had significantly stronger carboxylic (COOH) peaks that can be characteristic of polysaccharide diatom exudates [*Hawkins and Russell*, 2010; *Wilson et al.*, 2015], as well as carbonate (CO_3) peaks that could be biological [*Hawkins and Russell*, 2010] or from mineral dust from long-range transport (LRT). These differences were significant even when scaling by total carbon in individual particles. INPs also had significantly stronger alkyl (C-H) groups seen in some primary marine aerosol [*Hawkins and Russell*, 2010]; in combination with the carboxylic peaks these may represent long-chain fatty acids that have been implicated as one type of organic IN entity [*DeMott et al.*, 2018; *McCluskey et al.*, 2018a]. Finally, INPs had significantly stronger C=C peaks that may be indicative of polysaccharide-type marine emissions [*Hawkins and Russell*, 2010]. INPs also tended to have weaker carbonyl (C=O) peaks than the 150 m samples, however this latter difference was not significant at the 95% probability level. Above-cloud particles (n=24) had much stronger carbonate peaks than 500-m particles, likely due to the influence of mineral dust above the MBL. Like the INPs, they also had a significantly stronger alkyl signal. These statistics indicate that the INPs are quite different from most of the aerosol in the same size range near the ocean surface. Taken together with the STEM results (Figure 4), they suggest that biogenic marine compounds contribute to the small, but important INP population over the SO, with mineral dust and metals from long range transport contributing episodically in the free troposphere.

4. Discussion

4.1 Sources of Cloud Condensation Nuclei

In light of the high number fraction of sulfur-based particles in the 0.1-0.5 μm size range, both below and in-cloud, and their importance as CCN as discussed earlier, their sources are of interest. For the six below-cloud aerosol samples presented in section 3.1.1., the number concentration of small sulfur-based aerosols between about 0.08 μm-0.5 μm diameter (N_S) was approximated from the measured single-particle composition and the UHSAS number concentrations. (A lower size of 0.08 μm was used to include more of the aerosol accumulation mode, which tended to peak at ~0.10 μm.) Substantial variation in N_S was found for the different cases, ranging from a low of 29 cm^{-3} to a high of 224 cm^{-3}. HYSPLIT

back-trajectories (Figure S1) revealed that while most of the sampled airmasses came from the open ocean to the west, the two highest sulfur-based aerosol concentrations were associated with southerly trajectories that had recently passed over the Antarctic continent and high chlorophyll-a waters near the sea-ice edge (Figure 1). This suggests that many of the MB-CCN may derive from the Antarctic marginal sea-ice zone. In this region, large increases in DMS ocean concentrations [*Lana et al.*, 2011] and atmospheric flux [*Webb et al.*, 2019] have been observed, peaking in January/February, during the same season covered by the SOCRATES measurements. Southerly back-trajectories were also associated with the highest CCN number concentrations measured by the aircraft during the entire SOCRATES flight period [*McFarquhar et al.*, 2020; *Sanchez et al.*, 2021].

During a springtime cruise on an Australian icebreaker ship, *Humphries et al.* [2016] measured enhanced concentrations of >3 nm particles at high southern latitudes near East Antarctica. Based on airmass trajectories, they attributed the high particle concentrations to lofting of biogenic gases by the polar circulation to the free troposphere over Antarctica, new particle formation there, with subsequent descent back to the MBL related to cyclonic activity. The formation of new, ultrafine particles also has been observed directly in the summertime marine boundary layer in the Antarctic coastal zone where biological activity is enhanced [*Yu and Gan*, 2010; *Jokinen et al.*, 2018; *Jung et al.*, 2019]. The *Webb et al.* [2019] study found that DMS fluxes [*Pandis et al.*, 1994] were sufficient 63% of the time to produce new H_2SO_4 CCN under MBL conditions on the West Antarctic Peninsula. *Humphries et al.* [2015] documented a springtime new particle formation event within the Antarctic pack ice region that was initiated by a brief period of cloud clearing, which enhanced solar radiation and the opportunity for photochemical reactions.

Since sea-spray formation is supressed near the sea-ice edge and within ice leads [*Nilsson et al.*, 2001], pre-existing particle surface area can be lower near Antarctica than over open water elsewhere over the SO [*Yu and Gan*, 2010; *Humphries et al.*, 2015]. This and the low cold MBL temperatures could provide the opportunity for growth of recently formed particles via condensation of H_2SO_4 and MSA from oxidation of DMS to CCN-sized particles, aided by reactions in non-precipitating clouds [*Hoppel et al.*, 1994]. The latitudinal trend in mean annual precipitation rate over the SO determined from combined CloudSat/precipitation radar retrievals (2007-2009) peaks at ~40°S, decreases rapidly to ~50°S and then drops off more slowly farther poleward [*Behrangi et al.*, 2014]. Mean precipitation rate is ~30% less south of 60°S than between 50°S and 60°S, so less scavenging of CCN is expected over the SO near Antarctica. In addition, high-latitude precipitation tends to be in the form of snow rather than rain [*Behrangi et al.*, 2016], so nucleation scavenging will be suppressed. This increases the likelihood that particles nucleated in the MBL, or transported there after formation in the free troposphere, will survive to CCN sizes. Particles from the sea-ice zone over East Antarctica

592 can travel north to increase CCN concentrations over lower-productivity areas of the SO like
593 those sampled by the aircraft [*Humphries et al.*, 2016].

594 **4.2 Synthesis**

595 Based on the results from SOCRATES, CAPRICORN, and the other studies discussed,
596 Figure 5 shows a schematic overview of the major sources of cloud nucleating particles over
597 the SO between about 50°S and 70°S during the spring and summer months when much of
598 the sea-ice melts. In the generally low productivity region between 50-60°S, the main source
599 of cloud nucleating particles from the ocean surface is wind-driven sea-spray that produces
600 SS-CCN and sea-spray INPs (SS-INP), which may include marine micro-organisms. Some
601 biogenic gases condense on SS-CCN directly or through cloud processing in the MBL, but
602 weather disturbances favor lofting of precursor gases to colder, cleaner upper levels. Here,
603 exposed to ultraviolet radiation and in the low aerosol surface-area environment, they
604 condense to form new ultrafine particles over wide regions of the SO. These grow by
605 condensation and coagulation into primarily sulfur-based CCN that can form droplets directly
606 in mid-level clouds (particularly given the lack of SS-CCN, which leads to higher cloud
607 supersaturation in updrafts), or be entrained into the MBL and supplement SS-CCN as a
608 source of droplet nuclei in lower-level clouds. In the high productivity regions south of
609 ~62°S, MB-CCN may also form from new particle formation in the free troposphere or the
610 MBL, then grow in the MBL, particularly within the sea-ice zone. Formation and growth of
611 new CCN is favoured in this region due to strong biological activity and DMS flux, low sea-
612 spray surface area, and cold temperatures. Some of these CCN move with airmasses to lower
613 latitudes where they may nucleate clouds there.

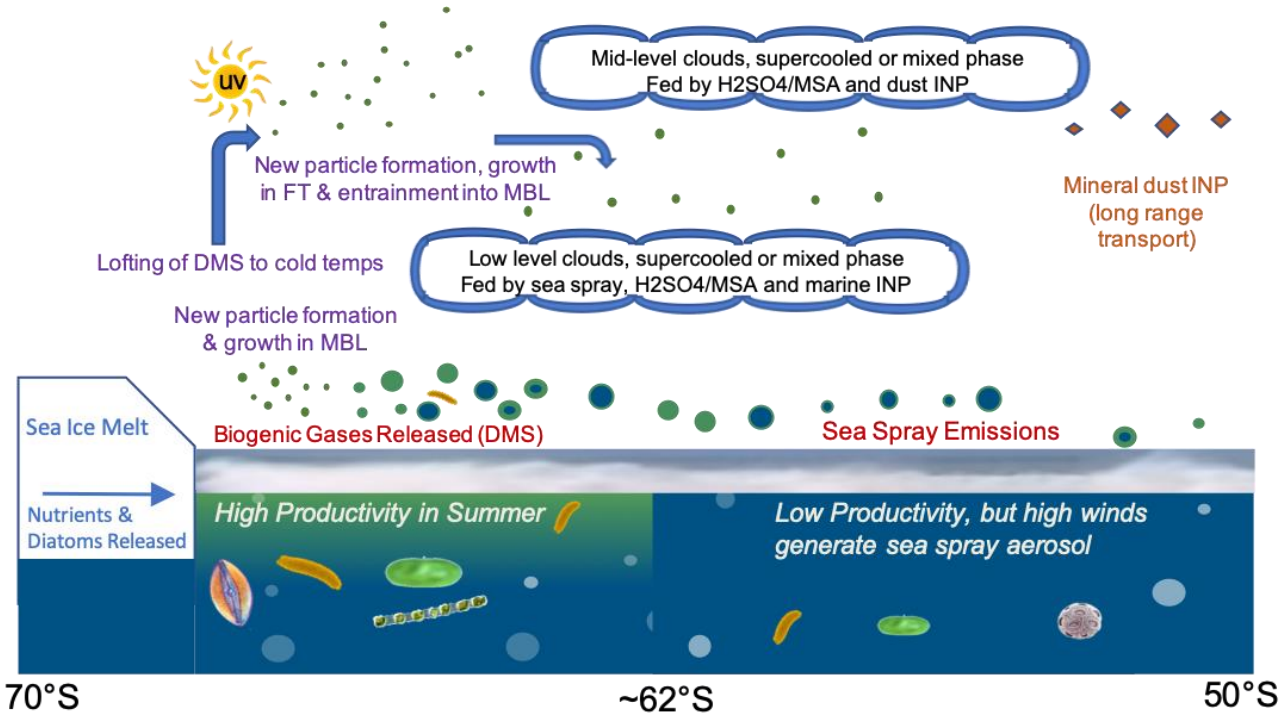

Figure 5. Schematic showing sources of cloud-nucleating aerosol particles over the Southern Ocean, with approximate latitudes for high (left) and low (right) productivity areas. The diagram depicts the austral spring and summer months when sea-ice melts and light levels are high, leading to phytoplankton blooms. MBL=Marine Boundary Layer and FT=Free Troposphere.

MBL clouds may remain supercooled until primary ice is formed, largely by nucleation of SS-INP. These nucleating particles may be enhanced over productive regions around Antarctica, but have a shorter lifetime than MB-CCN due to their larger size. Thus, they are less likely than MB-CCN to be carried to more northern latitudes to influence clouds there. MBL clouds may also be glaciated from ice falling from overlying mixed or ice-phase clouds. These mid-level clouds are likely influenced by mineral dust and metallic INPs which are the main type of large particles above the MBL and are efficient ice-nucleators at the cold temperatures aloft.

Not shown in Figure 5 are sinks of particles such as deposition, coagulation, and nucleation or impaction scavenging followed by precipitation, which are discussed in detail elsewhere [*Dunne et al.*, 2014]. Cloud-related sinks are expected to be reduced in summer months, when higher MB-CCN concentrations would lead to smaller droplets, reduced

coalescence/collision, and less rainfall. These effects are similar to those of enhanced concentrations of anthropogenic CCN documented in other studies [*Albrecht*, 1989; *Rosenfeld*, 2000; *Twohy et al.*, 2013].

5. Potential Climate Implications

Based on the information given above, the aerosol particle types that may be important for cloud formation over the SO are sea-spray CCN, biogenic sulfur-based CCN, sea-spray INPs, and mineral dust INPs (MD-INP). Using this and results from other studies, we consider below how number concentrations of each of these particle types may be impacted by physical factors such as higher surface winds and less sea ice expected in a changing climate. Also discussed are some studies showing aerosol changes in the warming Arctic, which has experienced substantial sea-ice loss already [*IPCC*, 2013]. It should be noted, however, that changes in Antarctic climate and sea-ice cover are more complex. Between 1979 and 2014, Antarctic sea ice extent actually slightly increased, then experienced a precipitous drop to below 1979 levels between 2015 and 2017 [*Parkinson*, 2019]. The recent changes are thought to be related to changes in atmospheric circulation which led to anomalous upper ocean temperatures in many Antarctic regions [*Meehl et al.*, 2019]. Despite these complicating effects, Antarctic sea ice is predicted to decrease by about 1/3 in response to greenhouse gas-induced warming by the year 2100 [*Bracegirdle et al.*, 2008] and to be nearly absent by 2300 [*Moore et al.*, 2018].

5.1 Potential Changes in Cloud Condensation Nuclei

5.1.1 Sea-spray CCN

Further modelled increases in the Southern Hemisphere's westerly jet may be partly offset by ozone recovery in lower CO_2 emissions scenarios, but surface windspeeds are predicted to increase 2-3 m/s by 2100 over the SO in the high emissions scenario [*Swart and Fyfe*, 2012]. In addition to the effect of increasing windspeed, sea-spray emissions are expected to increase as a consequence of the projected increased in ocean temperature and larger exposed ocean surface, effects that have been investigated for the Arctic [*Nilsson et al.*, 2001; *Struthers et al.*, 2011]. *Nilsson et al.* [2001] found that sea-spray flux over open ocean is about 10x higher than over open leads in Arctic sea ice, and calculated a large negative climate forcing through enhanced cloud albedo that may also occur over a future Southern Ocean. Note that all these effects are positive—i.e., SS-CCN emissions are expected to increase in number in a future climate, with potential increases in low-cloud albedo that have a cooling impact on climate.

Changes not only in SS-CCN source strength, but also in sinks may occur in a future climate. Precipitation is a significant CCN sink for marine low clouds in the current climate [*Wood et al.*, 2012], and could increase if clouds become more extensive or deeper in the future. However, the most recent climate models with more accurate cloud phase prediction show little change in SO low cloud cover or cloud thickness in a future climate [*Zelinka et al.*, 2020]. In one Arctic study using a detailed aerosol microphysics model, scavenging by drizzle was predicted to offset CCN increases from sea-ice loss [*Browse et al.*, 2014]. On the other hand, since more SS-CCN would produce more, smaller cloud droplets, drizzle could decrease in a future climate, extending the lifetime of SS-CCN. In the *Struthers et al.* [2011] Arctic climate simulations which included cloud microphysics impacts, the lifetime of sea-spray aerosol decreased due to enhanced wet scavenging, but was not sufficient to offset the enhanced cloud albedo effect. Thus we hypothesize that the overall effect of increasing SS-CCN still would be to increase cloud droplet concentration and cloud albedo. High emissions scenarios predict a windspeed increase of 2-3 m s^{-1} over the SO by years 2100-2300, with expected SS-CCN increases of 40-60% [*Dunne et al.*, 2014; *Moore et al.*, 2018].

5.1.2 Marine Biogenic CCN

Here we discuss the more complex questions of the types of changes that may be expected in MB-CCN over the future SO, and how these in turn might affect clouds and climate. Unlike the year-round effects of increasing winds on SS-CCN, future changes in MB-CCN are expected to occur primarily in the late spring through early fall season when temperature and light levels are high enough to favor biological activity and oxidation reactions. As with SS-CCN, higher windspeeds expected in a future climate can also impact MB-CCN. Stronger winds increase sea-air DMS flux and therefore gas to particle conversion. A mean 5% increase in MB-CCN is estimated already to have occurred between 1980 and 2002 due to this effect [*Korhonen et al.*, 2010], with impacts on cloud properties. Stronger winds also can enhance vertical mixing in the ocean, bringing nutrients to the surface where they can stimulate phytoplankton growth [*Ardyna et al.*, 2014].

Changes in DMS emissions and MB-CCN could also occur due to the ocean biota's response to myriad other climate-change impacts [*Cameron-Smith et al.*, 2011]. These include migration of water mass boundaries, warming temperatures, ocean acidification, increased cloud cover, glacial melt and sea-ice retreat, which in turn affect light availability and nutrient levels [*Deppeler and Davidson*, 2017]. A very complex ocean biogeochemistry-sea ice-atmosphere coupled model would be required to simulate all these factors and how they may impact clouds. Below we postulate on some of the major potential impacts.

In the Arctic, an approximately 50% increase in phytoplankton net primary productivity (NPP) has already been observed associated with regional warming and reduced sea-ice

extent over a 20-year period [*Arrigo and van Dijken*, 2015; *Kahru et al.*, 2016]. Higher NPP is associated with enhanced areas of open water, secondary blooms that occur in the fall [*Ardyna et al.*, 2014], a longer annual growing period [*Kahru et al.*, 2016], and blooms that occur at higher northern latitudes [*Renaut et al.*, 2018]. Arctic sea-ice decline correlates with increased ocean-to-atmosphere MSA and DMS emissions as well [*Sharma et al.*, 2012; *Galí et al.*, 2019]. Similarly, most earth system models also predict increasing biological activity in the Antarctic, poleward of 60°S [*Cabré et al.*, 2015; *Leung et al.*, 2015], where many summertime MB-CCN appear to be generated. This contrasts with decreased biological activity expected in ocean areas at lower latitudes. A coupled-climate model simulation run with a strong warming scenario predicted biological effects not only directly from warming oceans, but also from increased upwelling near the Antarctic continental shelf resulting from changes in atmospheric and ocean circulation and from increased light availability with less sea ice [*Moore et al.*, 2018]. These combined impacts are predicted to substantially increase phytoplankton primary productivity in the SO adjacent to the Antarctic continent, where nutrients become trapped along the coastal Antarctic waters and in the deep ocean.

Associated increases in annual primary production of about 20% are predicted by 2100 due to increased availability of light and iron near Antarctica [*Cabré et al.*, 2015; *Leung et al.*, 2015], with larger increases of about 50% by 2300 [*Moore et al.*, 2018]. That biological activity currently produces enhanced CCN and cloud droplet numbers in summer months over the SO is well established [*Ayers and Gras*, 1991; *Boers et al.*, 1998; *Yum and Hudson*, 2004; *Korhonen et al.*, 2008; *Gras and Keywood*, 2017]. Here we estimate that changes in MB-CCN are approximately proportional to modelled changes in primary productivity given at the beginning of this paragraph; i.e., 20% in 2100 and 50% in 2300. Taken together with expected increases in SS-CCN of 40-60% for 2100-2300, respectively (as discussed in the prior section), cloud-active CCN increases of 60-110% could occur over the SO in the future. A proportional increase in low cloud droplet number would lead to an increase in top-of-cloud (TOC) visible albedo of about 0.04-0.06 (*Charlson et al.* [1987], Figure 1; starting with a TOC albedo of 0.5 and assuming a constant liquid water path). As discussed below, such an albedo increase has the potential to partially, but not wholly, counteract the warming effects of loss of highly reflective sea-ice in a future climate: the so-called "ice-albedo feedback" [*Curry et al.*, 1995].

Frey et al. [2018] showed that Southern Ocean clouds are optically thicker over open ocean than over sea ice, an effect thought to be driven primarily by warmer temperatures producing thicker and more liquid-phase clouds. This effect has been predicted by models for a future climate [*J E Kay et al.*, 2016], but is not sufficient to offset the warming effects of losing sea ice since on average, the albedo associated with SO clouds over open water is smaller than the albedo over Antarctic sea ice. According to *Frey et al.* [2018], the top-of-atmosphere

(TOA) solar albedo is currently about 0.45 for clouds over open water, while it is about 0.61 for sea ice. Thus, more shortwave radiation would be absorbed when sea ice retreats and is replaced by clouds over open water. The potential TOC visible albedo increase of ~0.05 estimated above for increased CCN in the future corresponds to a TOA solar albedo increase of about 0.04 [*Charlson et al.*, 1987]. This is only ¼ of the expected TOA decrease due to sea ice loss. Thus enhanced CCN in a future climate are unlikely to balance the albedo decrease due to predicted Antarctic sea ice loss, but could partially offset it. Note that our estimates do not include potentially increasing sea-spray emissions due to more exposed ocean area, or any feedback of DMS-related cooling into sea-ice extent, as proposed by *Kim et al.* [2018].

5.2 Potential Changes in Ice Nucleating Particles

5.2.1 Sea-spray INPs

SS-INP are expected to be generated in higher concentrations as a result of increasing windspeeds. In addition, increased biological activity associated with Antarctic sea-ice retreat would likely produce more organic material in the sea-surface microlayer, which also could lead to more SS-INP. In the Arctic, increasingly common fractures (leads) in the sea-ice are correlated with enhanced organic material on SSA just after Arctic sunrise [*Kirpes et al.*, 2019]. More SS-INP potentially could result in more extensive mixed-phase and ice clouds in the Antarctic. In fact, satellite data compiled by *Listowski et al.* [2019] showed that Antarctic mixed phase clouds increase near the pole after summertime sea-ice retreat, and hypothesized that this was due to more marine INPs being emitted with increased biological activity in surface waters. However, an increase in INPs would be expected to have an opposite effect on cloud radiative properties to an increase in CCN. Ice in clouds grows at the expense of cloud droplets [*Storelvmo and Tan*, 2015], leading to lower surface area and clouds that are optically less dense. In addition, ice enhances precipitation processes in clouds, potentially decreasing their lifetime. Both these effects could have a climate warming impact, opposite of that of increasing CCN.

SS-INP are expected to increase due to the same processes that may influence SS-CCN and MB-CCN in a future climate—higher windspeeds and enhanced biological activity. A simple approximation would be that SS-INP would increase similarly in number to SS-CCN+MB-CCN, i.e., 60-110% for 2100 and 2300, respectively. This approximate doubling of SS-INP is unlikely to have as strong a radiative impact as doubling of CCN, however, because of the strong temperature dependence of INP activity. Since marine INP concentrations decrease by about a factor of 2 for each 1°C increase in cloud temperature [*DeMott et al.*, 2016; *McCluskey et al.*, 2018b], an increase in SS-INP number concentration of a factor of two would likely be completely offset by the 1-3°C temperature increase over the SO projected by 2100 [*Reisinger*, 2014]. This argument is consistent with the study of *Russell* [2015], who

predicted that mixed-phase clouds could be inhibited in the warmer boundary layers expected in a future climate. Thus, we hypothesize that the net effect of SS-INP changes on clouds in a warming climate would be small.

5.2.2 Mineral dust INPs

Changes in mineral dust INPs could affect cloud precipitation, optical properties and lifetime in similar ways as changes in SS-INP discussed above. Unfortunately, there is currently no consensus on how mineral dust loadings will change over the SO in the future, due to conflicting factors affecting emission and transport [*IPCC*, 2013]. For example, drought-related vegetation loss and increased storms producing higher winds could bring additional wind-blown dust to the SO [*Woodward et al.*, 2005]. However, CO_2 increases can also stimulate vegetation growth, while increasing storms may remove more dust from the atmosphere through wet deposition, for the opposite effect. Changes in atmospheric circulation could influence transport from continents to the remote SO as well. Thus more information is needed before any impact of changes in MD-INP on clouds over the SO reliably can be assessed. However, based on the temperature range of the low clouds sampled during SOCRATES (253K to 283K), only large increases in MD-INP could make them competitive with the more relevant SS-INP in this temperature range. This is because the major influence of mineral dust occurs below about 253K. Substantial increases in MD-INP might impact the properties of mid-level clouds, however. Also, increases in MD could have a secondary impact by depositing iron at the ocean surface. Since this nutrient is limited in many SO areas [*Deppeler and Davidson*, 2017], more iron could potentially impact future phytoplankton growth.

6 Summary

The two main CCN types in the summer MBL over the Southern Ocean in the sampled region are biogenic sulfur-based particles, which dominate the number concentration of particles 0.1-0.5 μm diameter, and sea-spray, which dominates particles >0.5 μm diameter. Compilation of data from this and other studies suggests that the Antarctic sea ice region is an important source of biogenic CCN in the summer months. Sulfate (and MSA) aerosol mass and CCN number are higher in the south near the Antarctic sea ice edge, where marine biological activity is enhanced in summer months. In this region the combination of high DMS flux, low sea-spray surface area, and cold temperatures can stimulate new particle production and growth, sometimes even in the marine boundary layer. Reduced precipitation in the Antarctic region relative to the open waters farther north can allow particles to grow to CCN sizes.

INPs are a different subset of the overall particle population, with STEM and STXM data showing that biogenic organics are important, with smaller contributions from mineral dust and metals from long-range transport which may be important at colder temperatures. The free troposphere over the SO has a variety of particle types, including small sulfur-based particles and larger mineral dust and metallic elements derived from long-range transport from the continents.

We hypothesize that most types of cloud nucleating particles, including sea-spray CCN, biogenic CCN, and sea-spray INP likely will increase in number over the SO in a future climate, while changes in mineral dust INP are harder to predict. The combined impact of increasing SS-CCN and MB-CCN could increase top-of-atmosphere albedo by approximately 0.04. This could partially but not completely offset the albedo decrease expected for a future loss of Antarctic sea-ice. The impact of changes in SS-INP is highly uncertain, but is expected to be smaller than the effects of CCN. We acknowledge that these are simple predictions for an extremely complex system. Detailed climate models that include impacts of ocean biology, air-sea interaction, and aerosol and cloud physical interactions are needed to test all aspects of this hypothesis.

Acknowledgements

The authors thank Cory Wolff and Pavel Romashkin, NCAR project managers, Mike Reeves, the crew of the NSF G-V aircraft, and SOCRATES PIs Greg McFarquhar, Chris Bretherton and Robert Wood, who provided useful support and suggestions. We also wish to thank the CSIRO Marine National Facility (MNF) for its support in the form of sea time on RV Investigator, support personnel, scientific equipment and data management, and lead CAPRICORN-2 scientist Alain Protat. All data and samples acquired on the voyage are made publicly available in accordance with MNF Policy. NASA OBPG provided the chlorophyll-a data used in Figure 1. NOAA Air Resources Laboratory provided the tools for the HYSPLIT trajectory analysis at https://ready.arl.noaa.gov/HYSPLIT.php. Much of this work was supported by the National Science Foundation; in particular CT was supported by NSF AGS-1660605 and DT and BR by NSF AGS-1660537. LR, SL, and KS used support from NSF AGS-1660509 for STXM analysis. KS and GR acknowledge the support of NSF AGS-1660374, and KM was supported by an NSF Graduate Research Fellowship under Grant No. 006784. Any opinions, findings, and conclusions or recommendations expressed in this material are those of the author(s) and do not necessarily reflect the views of the National Science Foundation. The authors declare that they have no conflict of interest.

Author contribution

CT led this research topic, compiled the STEM data, and was the primary author for the paper. DT and BW fielded the CVI instrumentation and helped collect and interpret data and samples. PD led the INP measurement effort, assisted by CM and KM and all helped with related sections of the paper. LR led the STXM analysis and helped with related sections of the paper. RG analyzed and interpreted STEM data. RH, PS, MK, JW and IM provided CCN and ACSM data and aided in its interpretation. CT, SL and KS helped with the STXM analysis and KS and GR also provided information on CCN sources and sinks.

Data availability

G-V aircraft state parameter and cloud physics data used are archived here: https://data.eol.ucar.edu/dataset/538.002, aircraft single particle STEM data here: https://data.eol.ucar.edu/dataset/552.131, and aircraft CCN data here: https://data.eol.ucar.edu/dataset/552.013. INP STEM data are here: https://doi.org/10.26023/THHB-X79P-A006, and STXM-NEXAFS data here: https://data.eol.ucar.edu/dataset/552.132 (or directly at https://library.ucsd.edu/dc/object/bb5398135k. CAPRICORN-2 aerosol composition and CCN data described in Section 3.1.2 are archived here: https://doi.org/10.25919/2h1c-t753. Chlorophyll-a data used in Figure 1 was obtained from the NASA Goddard Space Flight Center, Ocean Ecology Laboratory, Ocean Biology Processing Group (Moderate-resolution Imaging Spectroradiometer (MODIS) Aqua Chlorophyll Data; 2018 Reprocessing. NASA OB.DAAC, Greenbelt, MD, USA. doi: data/10.5067/AQUA/MODIS/L3M/CHL/2018. Accessed May 12, 2020).

References

Albrecht, B. (1989), Aerosols, cloud microphysics, and fractional cloudiness, *Science*, *245*(4923), 1227-1230.

Ardyna, M., M. Babin, M. Gosselin, E. Devred, L. Rainville, and J.-É. Tremblay (2014), Recent Arctic Ocean sea ice loss triggers novel fall phytoplankton blooms, *Geophys. Res. Lett.*, *41*(17), 6207-6212.

Arrigo, K. R., and G. L. van Dijken (2015), Continued increases in Arctic Ocean primary production, *Progress in Oceanography*, *136*, 60-70.

Ayers, G. P., and J. L. Gras (1991), Seasonal relationship between cloud condensation nuclei and aerosol methanesulphonate in marine air, *Nature*, *353*(6347), 834-835.

Bates, T. S., V. N. Kapustin, P. K. Quinn, D. S. Covert, D. J. Coffman, C. Mari, P. A. Durkee, W. J. De Bruyn, and E. S. Saltzman (1998), Processes controlling the distribution of aerosol particles in the lower marine boundary layer during the First Aerosol Characterization Experiment (ACE 1), *J. Geophys. Res. Atmos.*, *103*(D13), 16369-16383.

Behrangi, A., G. Stephens, R. F. Adler, G. J. Huffman, B. Lambrigtsen, and M. Lebsock (2014), An Update on the Oceanic Precipitation Rate and Its Zonal Distribution in Light of Advanced Observations from Space, *J. Climate*, *27*(11), 3957-3965.

881 Behrangi, A., et al. (2016), Status of High latitude precipitation estimates from observations and reanalyses, *J*
882 *Geophys Res Atmos*, *121*(9), 4468-4486.
883 Bigg, E. K. (1973), Ice Nucleus Concentrations in Remote Areas, *J. Atmos. Sci.*, *30*(6), 1153-1157.
884 Bigg, E. K., and C. Leck (2008), The composition of fragments of bubbles bursting at the ocean surface, *J.*
885 *Geophys. Res. Atmos.*, *113*(D11), n/a-n/a.
886 Bikkina, P., K. Kawamura, S. Bikkina, B. Kunwar, K. Tanaka, and K. Suzuki (2019), Hydroxy Fatty Acids in
887 Remote Marine Aerosols over the Pacific Ocean: Impact of Biological Activity and Wind Speed, *ACS Earth*
888 *and Space Chemistry*, *3*(3), 366-379.
889 Blanchard, D. C. (1964), Sea-to-Air Transport of Surface Active Material, *Science*, *146*(3642), 396.
890 Boers, R., J. B. Jensen, and P. B. Krummel (1998), Microphysical and short-wave radiative structure of
891 stratocumulus clouds over the Southern Ocean: Summer results and seasonal differences, *Q J Roy Meteor*
892 *Soc*, *124*(545), 151-168.
893 Bracegirdle, T. J., W. M. Connolley, and J. Turner (2008), Antarctic climate change over the twenty first
894 century, *J. Geophys. Res. Atmos.*, *113*(D3).
895 Browse, J., K. S. Carslaw, G. W. Mann, C. E. Birch, S. R. Arnold, and C. Leck (2014), The complex response
896 of Arctic aerosol to sea-ice retreat, *Atmos. Chem. Phys.*, *14*(14), 7543-7557.
897 Burrows, S. M., C. Hoose, U. Pöschl, and M. G. Lawrence (2013), Ice nuclei in marine air: biogenic particles or
898 dust?, *Atmos. Chem. Phys.*, *13*(1), 245-267.
899 Cabré, A., I. Marinov, and S. Leung (2015), Consistent global responses of marine ecosystems to future climate
900 change across the IPCC AR5 earth system models, *Climate Dynamics*, *45*(5-6), 1253-1280.
901 Cameron-Smith, P., S. Elliott, M. Maltrud, D. Erickson, and O. Wingenter (2011), Changes in dimethyl sulfide
902 oceanic distribution due to climate change, *Geophys. Res. Lett.*, *38*(7).
903 Charlson, R. J., J. E. Lovelock, M. O. Andreae, and S. G. Warren (1987), Oceanic phytoplankton, atmospheric
904 sulphur, cloud albedo and climate, *Nature*, *326*(6114), 655-661.
905 Chen, L., J. Wang, Y. Gao, G. Xu, X. Yang, Q. Lin, and Y. Zhang (2012), Latitudinal distributions of
906 atmospheric MSA and MSA/nss-SO42− ratios in summer over the high latitude regions of the Southern and
907 Northern Hemispheres, *J. Geophys. Res. Atmos.*, *117*(D10).
908 Chen, Q., T. Sherwen, M. Evans, and B. Alexander (2018), DMS oxidation and sulfur aerosol formation in the
909 marine troposphere: a focus on reactive halogen and multiphase chemistry, *Atmos. Chem. Phys.*, *18*(18),
910 13617-13637.
911 Clarke, A. D., and V. N. Kapustin (2002), A Pacific Aerosol Survey. Part I: A Decade of Data on Particle
912 Production, Transport, Evolution, and Mixing in the Troposphere, *J. Atmos. Sci.*, *59*(3), 363-382.
913 Clarke, A. D., Z. Li, and M. Litchy (1996), Aerosol dynamics in the equatorial Pacific marine boundary layer:
914 Microphysics, diurnal cycles and entrainment, *Geophys. Res. Lett.*, *23*(7), 733-736.
915 Craig, L., A. Moharreri, A. Schanot, D. C. Rogers, B. Anderson, and S. Dhaniyala (2013), Characterizations of
916 Cloud Droplet Shatter Artifacts in Two Airborne Aerosol Inlets, *Aerosol Sci Tech*, *47*(6), 662-671.
917 Curry, J. A., J. L. Schramm, and E. E. Ebert (1995), Sea Ice-Albedo Climate Feedback Mechanism, *J. Climate*,
918 *8*(2), 240-247.
919 Davison, B., C. O'Dowd, C. N. Hewitt, M. H. Smith, R. Harrison, D. A. Peel, E. Wolf, R. Mulvaney, M.
920 Schwikowski, and U. Baltenspergert (1996), Dimethyl sulfide and its oxidation products in the atmosphere
921 of the Atlantic and Southern Oceans, *Atmos. Environ.*, *30*, 1895-1906.
922 DeMott, P. J., et al. (2015), Integrating laboratory and field data to quantify the immersion freezing ice
923 nucleation activity of mineral dust particles, *Atmos. Chem. Phys.*, *15*(1), 393-409.
924 DeMott, P. J., et al. (2018), Ice Nucleation by Particles Containing Long-Chain Fatty Acids of Relevance to
925 Freezing by Sea Spray Aerosols, *Environ. Sci.: Processes Impact*, *20*(11), 1559−1569.

DeMott, P. J., et al. (2016), Sea spray aerosol as a unique source of ice nucleating particles, *Proceedings of the National Academy of Sciences*, *113*(21), 5797.
Deppeler, S. L., and A. T. Davidson (2017), Southern Ocean Phytoplankton in a Changing Climate, *Front. Mar. Sci.*, *4*, 40.
Després, V. R., et al. (2012), Primary biological aerosol particles in the atmosphere: a review, *Tellus B*, *64*(0).
Donahue, N. M., et al. How do organic vapors contribute to new-particle formation?(1359-6640 (Print)).
Dunne, E., S. Mikkonen, H. Kokkola, and H. Korhonen (2014), A global process-based study of marine CCN trends and variability, *Atmos Chem Phys*, *14*, 13631-13642.
Eastman, R., S. G. Warren, and C. J. q. Hahn (2014), Climatic Atlas of Clouds Over Land and Ocean, edited, https://atmos.uw.edu/CloudMap/.
Engström, A., F. A. M. Bender, R. J. Charlson, and R. Wood (2015), Geographically coherent patterns of albedo enhancement and suppression associated with aerosol sources and sinks, *Tellus B*, *67*(1), 26442.
Fossum, K. N., J. Ovadnevaite, D. Ceburnis, J. Preißler, J. R. Snider, R.-J. Huang, A. Zuend, and C. O'Dowd (2020), Sea-spray regulates sulfate cloud droplet activation over oceans, *npj Climate and Atmospheric Science*, *3*(1), 14.
Fossum, K. N., et al. (2018), Summertime Primary and Secondary Contributions to Southern Ocean Cloud Condensation Nuclei, *Sci. Rep.-UK*, *8*(1), 13844.
Frey, W. R., A. L. Morrison, J. E. Kay, R. Guzman, and H. Chepfer (2018), The Combined Influence of Observed Southern Ocean Clouds and Sea Ice on Top-of-Atmosphere Albedo, *J. Geophys. Res. Atmos.*, *123*(9), 4461-4475.
Fröhlich, R., et al. (2013), The ToF-ACSM: a portable aerosol chemical speciation monitor with TOFMS detection, *Atmos. Meas. Tech.*, *6*(11), 3225-3241.
Frossard, A. A., L. M. Russell, P. Massoli, T. S. Bates, and P. K. Quinn (2014), Side-by-Side Comparison of Four Techniques Explains the Apparent Differences in the Organic Composition of Generated and Ambient Marine Aerosol Particles, *Aerosol Sci Tech*, *48*(3), v-x.
Froyd, K. D., P. Yu, C. A. Brock, A. Kupc, D. M. Murphy, and C. J. Williamson (2020), Sources of Mineral Dust Aerosol to the Cirrus-Forming Regions of the Upper Troposphere, in *American Meteorological Society Annual Meeting*, edited, Boston, MA.
Galí, M., E. Devred, M. Babin, and M. Levasseur (2019), Decadal increase in Arctic dimethylsulfide emission, *Proceedings of the National Academy of Sciences*, *116*(39), 19311.
Gantt, B., N. Meskhidze, M. C. Facchini, M. Rinaldi, D. Ceburnis, and C. D. O'Dowd (2011), Wind speed dependent size-resolved parameterization for the organic mass fraction of sea spray aerosol, *Atmos. Chem. Phys.*, *11*(16), 8777-8790.
Gaston, C., H. Furutani, S. Guazzotti, K. Coffee, T. Bates, P. Quinn, L. Aluwihare, B. Mitchell, and K. Prather (2011), Unique ocean-derived particles serve as a proxy for changes in ocean chemistry, *J Geophys Res-Atmos*, *116*.
Gong, S. L. (2003), A parameterization of sea-salt aerosol source function for sub- and super-micron particles, *Global Biogeochem. Cyc.*, *17*(4).
Gras, J. L., and M. Keywood (2017), Cloud condensation nuclei over the Southern Ocean: wind dependence and seasonal cycles, *Atmos. Chem. Phys.*, *17*(7), 4419-4432.
Gray, A. R., K. S. Johnson, S. M. Bushinsky, S. C. Riser, J. L. Russell, L. D. Talley, R. Wanninkhof, N. L. Williams, and J. L. Sarmiento (2018), Autonomous Biogeochemical Floats Detect Significant Carbon Dioxide Outgassing in the High-Latitude Southern Ocean, *Geophys. Res. Lett.*, *45*(17), 9049-9057.
Gunson, J. R., S. A. Spall, T. R. Anderson, A. Jones, I. J. Totterdell, and M. J. Woodage (2006), Climate sensitivity to ocean dimethylsulphide emissions, *Geophys. Res. Lett.*, *33*(7).

971 Hande, L. B., S. T. Siems, and M. J. Manton (2012), Observed Trends in Wind Speed over the Southern Ocean,
972 *Geophys. Res. Lett.*, *39*(11).
973 Hawkins, L. N., and L. M. Russell (2010), Polysaccharides, proteins, and phytoplankton fragments: Four
974 chemically distinct types of marine primary organic aerosol classified by single particle spectromicroscopy,
975 *Advances in Meteorology*, *2010*, 14.
976 Heintzenberg, J., D. Covert, and R. Van Dingenen (2000), Size distribution and chemical composition of marine
977 aerosols: a compilation and review, *Tellus B*, *52B*, 1104-1122.
978 Hodshire, A. L., P. Campuzano-Jost, J. K. Kodros, B. Croft, B. A. Nault, J. C. Schroder, J. L. Jimenez, and J. R.
979 Pierce (2019), The potential role of methanesulfonic acid (MSA) in aerosol formation and growth and the
980 associated radiative forcings, *Atmos. Chem. Phys.*, *19*(5), 3137-3160.
981 Hoppel, W. A., G. M. Frick, J. W. Fitzgerald, and R. E. Larson (1994), Marine boundary layer measurements of
982 new particle formation and the effects nonprecipitating clouds have on aerosol size distribution, *J. Geophys.*
983 *Res. Atmos.*, *99*(D7), 14443-14459.
984 Huang, Y., S. Siems, M. Manton, A. Protat, and J. Delanoe (2012), A study on the low-altitude clouds over the
985 Southern Ocean using the DARDAR-MASK, *J. Geophys. Res. Atmos.*, *117*(D18).
986 Humphries, R. S., A. R. Klekociuk, R. Schofield, M. Keywood, J. Ward, and S. R. Wilson (2016), Unexpectedly
987 high ultrafine aerosol concentrations above East Antarctic sea ice, *Atmos. Chem. Phys.*, *16*(4), 2185-2206.
988 Humphries, R. S., I. M. McRobert, W. A. Ponsonby, J. P. Ward, M. D. Keywood, Z. M. Loh, P. B. Krummel,
989 and J. Harnwell (2019), Identification of platform exhaust on the RV Investigator, *Atmos. Meas. Tech.*,
990 *12*(6), 3019-3038.
991 Humphries, R. S., et al. (2015), Boundary layer new particle formation over East Antarctic sea ice – possible
992 Hg-driven nucleation?, *Atmos. Chem. Phys.*, *15*(23), 13339-13364.
993 IPCC (2013), Climate Change 2013: The Physical Science Basis*Rep.*, 1535 pp, Cambridge University Press,
994 Cambridge, United Kingdom and New York.
995 Jayarathne, T., et al. (2016), Enrichment of Saccharides and Divalent Cations in Sea Spray Aerosol During Two
996 Phytoplankton Blooms, *Environ Sci Technol*, *50*(21), 11511-11520.
997 Jickells, T. D., et al. (2005), Global iron donnections between desert dust, ocean biogeochemistry, and climate,
998 *Science*, *308*(5718), 67.
999 Jokinen, T., et al. (2018), Ion-induced sulfuric acid–ammonia nucleation drives particle formation in coastal
1000 Antarctica, *Science Advances*, *4*, eaat9744.
1001 Jung, J., et al. (2019), Characteristics of biogenically-derived aerosols over the Amundsen Sea, Antarctica,
1002 *Atmos. Chem. Phys. Discuss.*, *2019*, 1-37.
1003 Kahru, M., Z. Lee, B. G. Mitchell, and C. D. Nevison (2016), Effects of sea ice cover on satellite-detected
1004 primary production in the Arctic Ocean, *Biol Lett*, *12*(11), 20160223.
1005 Kay, J., L. Bourdages, N. B. Miller, A. Morrison, V. Yettella, H. Chepfer, and B. Eaton (2016), Evaluating and
1006 improving cloud phase in the Community Atmosphere Model version 5 using spaceborne lidar observations,
1007 *J. Geophys. Res. Atmos.*, *121*.
1008 Kay, J. E., C. Wall, V. Yettella, B. Medeiros, C. Hannay, P. Caldwell, and C. Bitz (2016), Global Climate
1009 Impacts of Fixing the Southern Ocean Shortwave Radiation Bias in the Community Earth System Model
1010 (CESM), *J. Climate*, *29*(12), 4617-4636.
1011 Keene, W. C., et al. (2007), Chemical and physical characteristics of nascent aerosols produced by bursting
1012 bubbles at a model air-sea interface, *J. Geophys. Res. Atmos.*, *112*(D21).
1013 Kim, A.-H., S. S. Yum, H. Lee, D. Chang, and S. Shim (2018), Polar Cooling Effect Due to Increase of
1014 Phytoplankton and Dimethyl-Sulfide Emission, *Atmosphere*, *9*(10), 384.

Kirpes, R. M., D. Bonanno, N. W. May, M. Fraund, A. J. Barget, R. C. Moffet, A. P. Ault, and K. A. Pratt (2019), Wintertime Arctic Sea Spray Aerosol Composition Controlled by Sea Ice Lead Microbiology, *ACS Central Science*.

Korhonen, H., K. S. Carslaw, D. V. Spracklen, G. W. Mann, and M. T. Woodhouse (2008), Influence of oceanic dimethyl sulfide emissions on cloud condensation nuclei concentrations and seasonality over the remote Southern Hemisphere oceans: A global model study, *J. Geophys. Res. Atmos.*, *113*(D15).

Korhonen, H., K. S. Carslaw, P. M. Forster, S. Mikkonen, N. D. Gordon, and H. Kokkola (2010), Aerosol climate feedback due to decadal increases in Southern Hemisphere wind speeds, *Geophys. Res. Lett.*, *37*(2).

Krüger, O., and H. Graßl (2011), Southern Ocean phytoplankton increases cloud albedo and reduces precipitation, *Geophys. Res. Lett.*, *38*(8).

Lana, A., et al. (2011), An updated climatology of surface dimethlysulfide concentrations and emission fluxes in the global ocean, *Global Biogeochem. Cyc.*, *25*(1).

Leung, S., A. Cabre, and I. Marinov (2015), A latitudinally banded phytoplankton response to 21st century climate change in the Southern Ocean across the CMIP5 model suite, *Biogeosciences*, *12*, 5715-5734.

Listowski, C., J. Delanoë, A. Kirchgaessner, T. Lachlan-Cope, and J. King (2019), Antarctic clouds, supercooled liquid water and mixed phase, investigated with DARDAR: geographical and seasonal variations, *Atmos. Chem. Phys.*, *19*(10), 6771-6808.

McCluskey, C. S., P. J. DeMott, P. L. Ma, and S. M. Burrows (2019), Numerical Representations of Marine Ice-Nucleating Particles in Remote Marine Environments Evaluated Against Observations, *Geophys. Res. Lett.*, *46*(13), 7838-7847.

McCluskey, C. S., et al. (2018a), A Mesocosm Double Feature: Insights into the Chemical Makeup of Marine Ice Nucleating Particles, *J. Atmos. Sci.*, *75*(7), 2405-2423.

McCluskey, C. S., et al. (2018b), Observations of Ice Nucleating Particles Over Southern Ocean Waters, *Geophys. Res. Lett.*, *45*(21), 11,989-911,997.

McCoy, D. T., S. M. Burrows, R. Wood, D. P. Grosvenor, S. M. Elliott, P.-L. Ma, P. J. Rasch, and D. L. Hartmann (2015), Natural aerosols explain seasonal and spatial patterns of Southern Ocean cloud albedo, *Science Advances*, *1*(6), e1500157.

McCoy, I. L., C. S. Bretherton, R. Wood, C. H. Twohy, A. Gettelman, C. G. Bardeen, and D. W. Toohey (2021), Recent particle formation and aerosol variability near Southern Ocean low clouds, *J. Geophys. Res.*, *under review, Preprint available at https://www.essoar.org/doi/10.1002/essoar.10503719.1*.

McFarquhar, G. M., et al. (2020), Observations of clouds, aerosols, precipitation, and surface radiation over the Southern Ocean: An overview of CAPRICORN, MARCUS, MICRE and SOCRATES, *B Am Meteorol Soc*, 1-92.

McInnes, L. M., D. Covert, P. K. Quinn, and M. S. Germani (1994), Measurements of chloride depletion and sulfur enrichment in individual sea-salt particles collected from the remote marine boundary layer, *J. Geophys. Res. Atmos.*, *99*(D4), 8257-8268.

Meehl, G. A., J. M. Arblaster, C. T. Y. Chung, M. M. Holland, A. DuVivier, L. Thompson, D. Yang, and C. M. Bitz (2019), Sustained ocean changes contributed to sudden Antarctic sea ice retreat in late 2016, *Nat. Comm.*, *10*(1), 14.

Middlebrook, A. M., D. M. Murphy, and D. S. Thomson (1998), Observations of organic material in individual marine particles at Cape Grim during the First Aerosol Characterization Experiment (ACE 1), *J. Geophys. Res. Atmos.*, *103*(D13), 16475-16483.

Moore, J. K., W. Fu, F. Primeau, G. L. Britten, K. Lindsay, M. Long, S. C. Doney, N. Mahowald, F. Hoffman, and J. T. Randerson (2018), Sustained climate warming drives declining marine biological productivity, *Science*, *359*(6380), 1139.

Murray, B. J., D. O'Sullivan, J. D. Atkinson, and M. E. Webb (2012), Ice nucleation by particles immersed in supercooled cloud droplets, *Chemical Society Reviews*, *41*(19), 6519-6554.
Neff, P. D., and N. A. N. Bertler (2015), Trajectory modeling of modern dust transport to the Southern Ocean and Antarctica, *J. Geophys. Res. Atmos.*, *120*(18), 9303-9322.
Nilsson, E. D., Ü. Rannik, E. Swietlicki, C. Leck, P. P. Aalto, J. Zhou, and M. Norman (2001), Turbulent aerosol fluxes over the Arctic Ocean: 2. Wind-driven sources from the sea, *J. Geophys. Res. Atmos.*, *106*(D23), 32139-32154.
Noone, K. J., J. A. Ogren, J. Heintzenberg, R. J. Charlson, and D. S. Covert (1988), Design and calibration of a Counterflow Virtual Impactor for sampling of atmospheric fog and cloud droplets, *Aerosol Sci. Technol.*, *8*(3), 235-244.
O'Dowd, C. D., M. H. Smith, I. E. Consterdine, and J. A. Lowe (1997a), Marine aerosol, sea-salt, and the marine sulphur cycle: a short review, *Atmos. Environ.*, *31*(1), 73-80.
O'Dowd, C. D., J. A. Lowe, M. H. Smith, B. Davison, C. N. Hewitt, and R. M. Harrison (1997b), Biogenic sulphur emissions and inferred non-sea-salt-sulphate cloud condensation nuclei in and around Antarctica, *J. Geophys. Res. Atmos.*, *102*(D11), 12839-12854.
O'Dowd, C. D., M. C. Facchini, F. Cavalli, D. Ceburnis, M. Mircea, S. Decesari, S. Fuzzi, Y. J. Yoon, and J.-P. Putaud (2004), Biogenically driven organic contribution to marine aerosol, *Nature*, *431*(7009), 676-680.
O'Dowd, C. D., J. L. Jimenez, R. Bahreini, R. C. Flagan, J. H. Seinfeld, K. Hämeri, L. Pirjola, M. Kulmala, S. G. Jennings, and T. Hoffmann (2002), Marine aerosol formation from biogenic iodine emissions, *Nature*, *417*(6889), 632-636.
Pandis, S. N., L. M. Russell, and J. H. Seinfeld (1994), The relationship between DMS flux and CCN concentration in remote marine regions, *J. Geophys. Res. Atmos.*, *99*(D8), 16945-16957.
Parkinson, C. L. (2019), A 40-y record reveals gradual Antarctic sea ice increases followed by decreases at rates far exceeding the rates seen in the Arctic, *Proceedings of the National Academy of Sciences*, *116*(29), 14414.
Petrou, K., and P. J. Ralph (2011), Photosynthesis and net primary productivity in three Antarctic diatoms: possible significance for their distribution in the Antarctic marine ecosystem, *Marine Ecology Progress Series*, *437*, 27-40.
Pierce, J. R., and P. J. Adams (2006), Global evaluation of CCN formation by direct emission of sea salt and growth of ultrafine sea salt, *J. Geophys. Res. Atmos.*, *111*(D6).
Platnick, S., and S. Twomey (1994), Determining the Susceptibility of Cloud Albedo to Changes in Droplet Concentration with the Advanced Very High Resolution Radiometer, *J. Appl. Meteorol.*, *33*(3), 334-347.
Quinn, P. K., D. J. Coffman, J. E. Johnson, L. M. Upchurch, and T. S. Bates (2017), Small fraction of marine cloud condensation nuclei made up of sea spray aerosol, *Nat Geosci*, *10*, 674.
Quinn, P. K., et al. (2000), Surface submicron aerosol chemical composition: What fraction is not sulfate?, *J. Geophys. Res. Atmos.*, *105*(D5), 6785-6805.
Radhi, M. (2010), Physical and Chemical Properties of Australian Continental Aerosols, Ph. D. thesis, 197 pp, University of New South Wales, Sydney, Australia.
Read, K. A., et al. (2008), DMS and MSA measurements in the Antarctic Boundary Layer: impact of BrO on MSA production, *Atmos. Chem. Phys.*, *8*(11), 2985-2997.
Reisinger, A., R.L. Kitching, F. Chiew, L. Hughes, P.C.D. Newton, S.S. Schuster, A. Tait, and P. Whetton (2014), Australasia. In: Climate Change 2014: Impacts, Adaptation, and Vulnerability. Part B: Regional Aspects. Contribution of Working Group II to the Fifth Assessment Report of the Intergovernmental Panel on Climate Change*Rep.*, 1371-1438 pp, Cambridge University Press, Cambridge, United Kingdom and New York.
Renaut, S., E. Devred, and M. Babin (2018), Northward Expansion and Intensification of Phytoplankton Growth During the Early Ice-Free Season in Arctic, *Geophys. Res. Lett.*, *45*(19), 10,590-510,598.

1106 Rosenfeld, D. (2000), Suppression of Rain and Snow by Urban and Industrial Air Pollution, *Science*, *287*(5459),
1107 1793.
1108 Russell, L., L. N. Hawkins, A. A. Frossard, P. K. Quinn, and T. S. Bates (2010), Carbohydrate-like composition
1109 of submicron atmospheric particles and their production from ocean bubble bursting, *P Natl Acad Sci USA*,
1110 *107*(15), 16652–16657.
1111 Russell, L. M. (2015), Sea-spray particles cause freezing in clouds, *Nature*, *525*, 194.
1112 Saiz-Lopez, A., A. S. Mahajan, R. A. Salmon, S. J. B. Bauguitte, A. E. Jones, H. K. Roscoe, and J. M. C. Plane
1113 (2007), Boundary Layer Halogens in Coastal Antarctica, *Science*, *317*(5836), 348.
1114 Saliba, G., et al. (2020), Organic composition of three different size ranges of aerosol particles over the
1115 Southern Ocean, *Aerosol Sci Tech*, 1-25.
1116 Salter, M. E., E. Hamacher-Barth, C. Leck, J. Werner, C. M. Johnson, I. Riipinen, E. D. Nilsson, and P. Zieger
1117 (2016), Calcium enrichment in sea spray aerosol particles, *Geophys. Res. Lett.*, *43*(15), 8277-8285.
1118 Sanchez, K. J., G. C. Roberts, G. Saliba, L. M. Russell, C. H. Twohy, J. M. Reeves, R. S. Humphries, M.
1119 Keywood, J. Ward, and I. McRobert (2021), Measurement Report: Cloud Processes and the Transport of
1120 Biological Emissions Affect Southern Ocean Particle and Cloud Condensation Nuclei Concentrations,
1121 *Atmos. Chem. Phys., in press.*
1122 Schmale, J., et al. (2019), Overview of the Antarctic Circumnavigation Expedition: Study of Preindustrial-like
1123 Aerosols and Their Climate Effects (ACE-SPACE), *B Am Meteorol Soc*, *100*(11), 2260-2283.
1124 Sharma, S., et al. (2012), Influence of transport and ocean ice extent on biogenic aerosol sulfur in the Arctic
1125 atmosphere, *J. Geophys. Res. Atmos.*, *117*(D12).
1126 Smetacek, V., and S. Nicol (2005), Polar ocean ecosystems in a changing world, *Nature*, *437*(7057), 362-368.
1127 Song, C. H., and G. R. Carmichael (1999), The aging process of naturally emitted aerosol (sea-salt and mineral
1128 aerosol) during long range transport, *Atmos. Environ.*, *33*(14), 2203-2218.
1129 Storelvmo, T., and I. Tan (2015), The Wegener-Bergeron-Findeisen process ? Its discovery and vital importance
1130 for weather and climate, *Meteorologische Zeitschrift*, *24*(4), 455-461.
1131 Struthers, H., A. M. L. Ekman, P. Glantz, T. Iversen, A. Kirkevåg, E. M. Mårtensson, Ø. Seland, and E. D.
1132 Nilsson (2011), The effect of sea ice loss on sea salt aerosol concentrations and the radiative balance in the
1133 Arctic, *Atmos. Chem. Phys.*, *11*(7), 3459-3477.
1134 Swart, N. C., and J. C. Fyfe (2012), Observed and simulated changes in the Southern Hemisphere surface
1135 westerly wind-stress, *Geophys. Res. Lett.*, *39*(16).
1136 Tremblay, J.-É., and J. Gagnon (2009), The effects of irradiance and nutrient supply on the productivity of
1137 Arctic waters: a perspective on climate change, in *Influence of Climate Change on the Changing Arctic and*
1138 *Sub-Arctic Conditions*, edited by J. C. J. Nihoul and A. G. Kostianoy, pp. 73-93, Springer Netherlands,
1139 Dordrecht.
1140 Trenberth, K. E., and J. T. Fasullo (2010), Simulation of Present-Day and Twenty-First-Century Energy Budgets
1141 of the Southern Oceans, *J. Climate*, *23*(2), 440-454.
1142 Twohy, C. H., P. H. Austin, and R. J. Charlson (1989), Chemical consequences of the initial diffusional growth
1143 of cloud droplets: a clean marine case, *Tellus B*, *41*(1), 51-60.
1144 Twohy, C. H., J. W. Strapp, and M. Wendisch (2003), Performance of a counterflow virtual impactor in the
1145 NASA Icing Research Tunnel, *J. Atmos. Ocean. Tech.*, *20*(6), 781-790.
1146 Twohy, C. H., G. R. McMeeking, P. J. DeMott, C. S. McCluskey, T. C. J. Hill, S. M. Burrows, G. R. Kulkarni,
1147 M. Tanarhte, D. N. Kafle, and D. W. Toohey (2016), Abundance of fluorescent biological aerosol particles
1148 at temperatures conducive to the formation of mixed-phase and cirrus clouds, *Atmos. Chem. Phys.*, *16*(13),
1149 8205-8225.
1150 Twohy, C. H., et al. (2013), Impacts of aerosol particles on the microphysical and radiative properties of
1151 stratocumulus clouds over the southeast Pacific Ocean, *Atmos Chem Phys*, *13*(5), 2541-2562.

Vallina, S. M., R. Simó, and S. Gassó (2006), What controls CCN seasonality in the Southern Ocean? A statistical analysis based on satellite-derived chlorophyll and CCN and model-estimated OH radical and rainfall, *Global Biogeochem. Cyc.*, *20*(1).
Vergara-Temprado, J., A. K. Miltenberger, K. Furtado, D. P. Grosvenor, B. J. Shipway, A. A. Hill, J. M. Wilkinson, P. R. Field, B. J. Murray, and K. S. Carslaw (2018), Strong control of Southern Ocean cloud reflectivity by ice-nucleating particles, *Proceedings of the National Academy of Sciences*, *115*(11), 2687.
Wang, H., et al. (2020), Aerosols in the E3SM Version 1: New Developments and Their Impacts on Radiative Forcing, *Journal of Advances in Modeling Earth Systems*, *12*(1), e2019MS001851.
Wang, S., M. E. Maltrud, S. M. Burrows, S. M. Elliott, and P. Cameron-Smith (2018), Impacts of Shifts in Phytoplankton Community on Clouds and Climate via the Sulfur Cycle, *Global Biogeochem. Cyc.*, *32*(6), 1005-1026.
Webb, A. L., M. A. van Leeuwe, D. den Os, M. P. Meredith, H. J. Venables, and J. Stefels (2019), Extreme spikes in DMS flux double estimates of biogenic sulfur export from the Antarctic coastal zone to the atmosphere, *Sci. Rep.-UK*, *9*(1), 2233.
Westwood, K. J., P. G. Thomson, R. L. van den Enden, L. E. Maher, S. W. Wright, and A. T. Davidson (2018), Ocean acidification impacts primary and bacterial production in Antarctic coastal waters during austral summer, *Journal of Experimental Marine Biology and Ecology*, *498*, 46-60.
Wilson, T. W., et al. (2015), A marine biogenic source of atmospheric ice-nucleating particles, *Nature*, *525*(7568), 234-238.
Wood, R., D. Leon, M. Lebsock, J. Snider, and A. D. Clarke (2012), Precipitation driving of droplet concentration variability in marine low clouds, *J. Geophys. Res. Atmos.*, *117*(D19).
Woodward, S., D. L. Roberts, and R. A. Betts (2005), A simulation of the effect of climate change–induced desertification on mineral dust aerosol, *Geophys. Res. Lett.*, *32*(18).
Xu, G., Y. Gao, Q. Lin, W. Li, L. Chen, C. Xu, Y. Gao, Q. Lin, W. Li, and L. Chen (2013), Characteristics of water-soluble inorganic and organic ions in aerosols over the Southern Ocean and coastal East Antarctica during austral summer: AEROSOL IN SOUTHERN OCEAN AND ANTARCTICA, *J. Geophys. Res. Atmos.*, *118*.
Xu, L., D. W. Pierce, L. M. Russell, A. J. Miller, R. C. J. Somerville, C. H. Twohy, S. J. Ghan, B. Singh, J.-H. Yoon, and P. J. Rasch (2015), Interannual to decadal climate variability of sea salt aerosols in the coupled climate model CESM1.0, *J. Geophys. Res. Atmos.*, *120*(4), 1502-1519.
Young, I. R., and A. Ribal (2019), Multiplatform evaluation of global trends in wind speed and wave height, *Science*, *364*(6440), 548.
Yu, F., and L. Gan (2010), Oceanic Dimethyl Sulfide Emission and New Particle Formation around the Coast of Antarctica: A Modeling Study of Seasonal Variations and Comparison with Measurements, *Atmosphere*, *1*.
Yum, S. S., and J. G. Hudson (2004), Wintertime/summertime contrasts of cloud condensation nuclei and cloud microphysics over the Southern Ocean, *J. Geophys. Res. Atmos.*, *109*(D6).
Zelinka, M. D., T. A. Myers, D. T. McCoy, S. Po-Chedley, P. M. Caldwell, P. Ceppi, S. A. Klein, and K. E. Taylor (2020), Causes of Higher Climate Sensitivity in CMIP6 Models, *Geophys. Res. Lett.*, *47*(1), e2019GL085782.
Zhao, X., X. Liu, S. Burrows, and Y. Shi (2020), Effects of Marine Organic Aerosols as Sources of Immersion-Mode Ice Nucleating Particles on High Latitude Mixed-Phase Clouds, *Atmos. Chem. Phys. Discuss.*, *2020*, 1-49.